

REVIEW ARTICLE

10.1029/2018RG000598

Key Points:

- Satellite-based optical sensors are an efficient means for observing surface water regionally and globally
- Pixel unmixing and reconstruction, and spatio-temporal fusion are two common and low-cost approaches to enhance surface water monitoring
- The potential to estimate flow using only optical remote sensing has greatly enriched the data source of hydrological studies

Correspondence to:

C. Huang,
changh@nwu.edu.cn

Citation:

Huang, C., Chen, Y., Zhang, S., & Wu, J. (2018). Detecting, extracting, and monitoring surface water from space using optical sensors: A review. *Reviews of Geophysics*, 56, 333–360. <https://doi.org/10.1029/2018RG000598>

Received 18 JAN 2018

Accepted 11 MAY 2018

Accepted article online 21 MAY 2018

Published online 6 JUN 2018

Detecting, Extracting, and Monitoring Surface Water From Space Using Optical Sensors: A Review

Chang Huang^{1,2} , Yun Chen³, Shiqiang Zhang^{1,2}, and Jianping Wu⁴

¹Shaanxi Key Laboratory of Earth Surface System and Environmental Carrying Capacity, Northwest University, Xi'an, China,

²College of Urban and Environmental Sciences, Northwest University, Xi'an, China, ³Commonwealth Scientific and Industrial Research Organisation Land and Water, Canberra, ACT, Australia, ⁴Key Laboratory of Geographic Information Science, Ministry of Education, East China Normal University, Shanghai, China

Abstract Observation of surface water is a functional requirement for studying ecological and hydrological processes. Recent advances in satellite-based optical remote sensors have promoted the field of sensing surface water to a new era. This paper reviews the current status of detecting, extracting, and monitoring surface water using optical remote sensing, especially progress in the last decade. It also discusses the current status and challenges in this field, including spatio-temporal scale issues, integration with in situ hydrological data and elevation data, obscuration caused by clouds and vegetation, and the growing need to map surface water at a global scale. Historically, sensors have exhibited a contradiction in resolutions. Techniques including pixel unmixing and reconstruction, and spatio-temporal fusion have been developed to alleviate this contradiction. Spatio-temporal dynamics of surface water have been modeled by combining remote sensing data with in situ river flow. Recent studies have also demonstrated that the river discharge can be estimated using only optical remote sensing imagery, providing valuable information for hydrological studies in ungauged areas. Another historical issue for optical sensors has been obscuration by clouds and vegetation. An effective approach of reducing this limitation is to combine with synthetic aperture radar data. Digital elevation model data have also been employed to eliminate cloud/terrain shadows. The development of big data and cloud computation techniques makes the increasing demand of monitoring global water dynamics at high resolutions easier to achieve. An integrated use of multisource data is the future direction for improved global and regional water monitoring.

Plain Language Summary Observing surface water is essential for ecological and hydrological studies. This paper reviews the current status of detecting, extracting, and monitoring surface water using optical remote sensing, especially progress in the last decade. It also discusses the current status and challenges in this field. For example, it was found that pixel unmixing and reconstruction, and spatio-temporal fusion are two common and low-cost approaches to enhance surface water monitoring. Remote sensing data have been integrated with in situ river flow to model spatio-temporal dynamics of surface water. Recent studies have also proved that the river discharge can be estimated using only optical remote sensing imagery. This will be a breakthrough for hydrological studies in ungauged areas. Optical sensors are also easily obscured by clouds and vegetation. This limitation can be reduced by integrating optical data with synthetic aperture radar data and digital elevation model data. There is increasing demand of monitoring global water dynamics at high resolutions. It is now easy to achieve with the development of big data and cloud computation techniques. Enhanced global or regional water monitoring in the future requires integrated use of multiple sources of remote sensing data.

1. Introduction

Surface water refers to water on the surface of the Earth, such as a river, lake, wetland, and the ocean. Usually, the ocean is excluded in the definition because it is so large and because it is salty, though smaller saline water bodies are usually included. This definition is adopted in this review. Surface water bodies are critical freshwater resources, for both human and ecological systems. They are of paramount importance in sustaining all forms of lives (Karpalne et al., 2016). Water helps preserve the biodiversity in riparian or wetland ecosystems by providing habitats to a plethora of flora and fauna (Vörösmarty et al., 2010). It is not only critical to the ecosystems as a key component of the hydrologic cycle but also touches every aspect of our lives, such as drinking water, agriculture, electricity production, transportation, and industrial purposes (Vörösmarty et al., 2000).

©2018. The Authors.

This is an open access article under the terms of the Creative Commons Attribution-NonCommercial-NoDerivs License, which permits use and distribution in any medium, provided the original work is properly cited, the use is non-commercial and no modifications or adaptations are made.

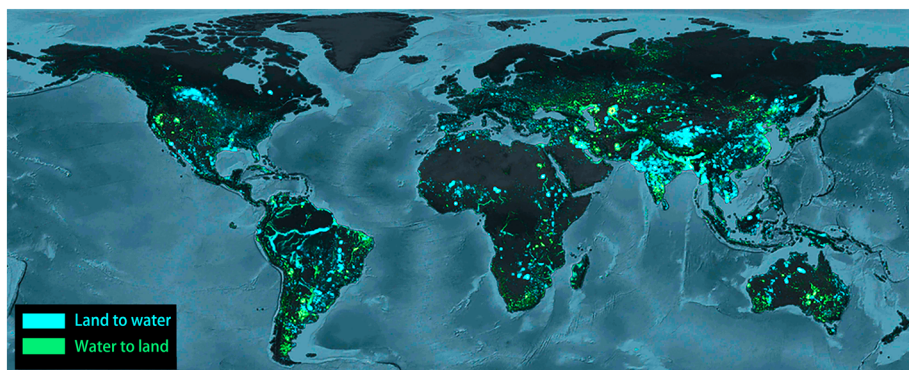


Figure 1. Heat map of global surface water and land changes (figure reprinted from Donchyts et al., 2016).

Surface water bodies are dynamic in nature as they shrink, expand, or change their appearance or course of flow with time, owing to different natural and human-induced factors (Karpatne et al., 2016). Variations in water bodies impact other natural resources and human assets and further influence the environment. Change in surface water volume usually causes serious consequences. In extreme cases, rapid increase of surface water can result in flooding. Therefore, it is crucial to efficiently detect the existence of surface water, to extract its extent, to quantify its volume, and to monitor its dynamics.

Remote sensing technology offers effective ways to observe surface water dynamics. Compared to traditional in situ measurements, remote sensing is much more efficient, because of its ability to continuously monitor Earth's surface at multiple scales. Remote sensing data sets provide spatially explicit and temporally frequent observational data of a number of physical attributes about the Earth's surface that can be appropriately leveraged to map the extent of water bodies at regional or even global scale, and to monitor their dynamics at regular and frequent time intervals. As an example of water dynamics, Figure 1 shows a heat map of global surface water and land changes over the period 1985–2015, generated using Landsat images (Donchyts et al., 2016). The blue lighting shows where land was converted to water, while the green lighting shows where water was converted to land during this period. The intensity of the colors highlights the spatial magnitude of the change.

There are generally two categories of sensors that can serve the purpose of measuring surface water—the optical sensor and the microwave sensor. Microwave sensors, due to their usage of long wavelength radiation, have the ability to penetrate cloud coverage and certain vegetation coverage. Independent of solar radiation, they can work day and night under any weather condition. Schumann and Moller (2015) conducted a detailed review of microwave remote sensing for flood inundation and found synthetic aperture radar (SAR) to be the most suitable microwave sensor type for monitoring flood inundation. Optical sensors, which are the focus of this review, have been widely applied in this field due to high data availability, as well as suitable spatial and temporal resolutions (Huang et al., 2015). Bhavasar (1984) published a review on the applications of remote sensing technology to hydrology and water resources management in India as early as 1984, when remote sensing was still at its very early stage. Smith (1997) conducted a comprehensive review after more than a decade, in which he introduced many representative studies that used satellite remote sensing data to derive river inundation area, stage, and discharge. Alsdorf and Lettenmaier (2003) depicted a large picture on tracking fresh water from space in *Science* magazine, and later in 2007, they made a much more detailed review of all kinds of remote sensing approaches for measuring surface water (Alsdorf et al., 2007). Schumann et al. (2009) introduced methods of deriving flood extent using remote sensing, but they focused more on the integration of flood extent and hydraulic models. We surveyed the Web of Knowledge database (Web of Science Core Collection) for papers published in relevant areas since 2000, which had the term "surface water" or "flood inundation" in their topic, refined by the term "remote sensing" (Figure 2). Since 2000, the number of studies that used remote sensing to research on surface water and flood inundation has increased steadily, with the last decade showing a threefold to sevenfold increase.

To demonstrate how the use of remote sensing has advanced surface water and flood inundation studies, this review tracks the latest progress in measuring surface water using satellite-based optical sensors, especially those works that have been conducted in the last decade. Current status and challenges in this field,

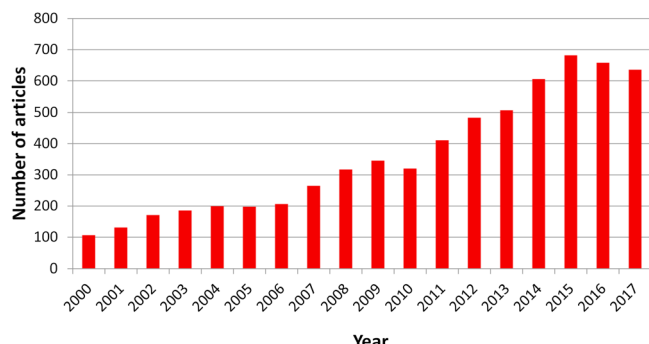


Figure 2. Number of published articles (2000–2017) listed in Web of Science Core Collection containing the terms “surface water” or “flood inundation,” and refined by “remote sensing.”

including spatio-temporal scale issues, integration with in situ hydrological data and elevation data, obscuration caused by clouds and vegetation, and the growing need for mapping surface water globally, are also discussed in details, in order to further encourage studies in the related field. Sensors for surface water detection and methods for surface water extraction are covered in sections 2 and 3. Spatial and temporal monitoring of surface water is discussed in section 4. Some particular challenges and limitations regarding remote sensing of surface water are presented in section 5. Finally, conclusions are drawn and prospective future research is identified in section 6.

2. Detection of Surface Water With Different Sensors

Since the first Earth Resources Technology Satellite (ERTS-1, later renamed as Landsat-1) was launched in 1972, satellite-based optical

sensors have demonstrated their potential to monitor large-scale land cover change on the Earth’s surface (Deutsch & Ruggles, 1974). As a significant land cover change phenomenon, surface water dynamics have always been an important topic of Earth observation (e.g., Sakamoto et al., 2007; Schaffer-Smith et al., 2017). Spatial resolution refers to the area of ground observed within a pixel and determines the level of details captured by the sensors. As it is one of the most direct factors that control the usage of different sensors in the applications of detecting surface water, we have used spatial resolution to categorize optical sensors into three groups—coarse (>200 m), medium (5–200 m), and high (<5 m).

2.1. Coarse Spatial Resolution Sensors

Coarse-resolution remote sensors have the inherent defect of low accuracy due to their high information generalization level, but they usually have the characteristics of a high temporal resolution and a broad coverage. A typical example is the Advanced Very High Resolution Radiometer onboard National Oceanic and Atmospheric Administration satellites (NOAA/AVHRR). This sensor was originally designed to monitor the ocean and atmosphere but was later found to also be effective in detecting large-scale flood events (Barton & Bathols, 1989). After that, more and more studies have examined the ability of NOAA/AVHRR to detect flood inundation (Domenikiotis et al., 2003; Islam & Sado, 2000; Jain et al., 2006; Nyborg & Sandholt, 2001; Sheng et al., 2001; Zhou, 2000). Like all other optical sensors, NOAA/AVHRR suffers from the cloud contamination problem (Sheng et al., 1998), especially the wide distribution of clouds during flood events.

The Moderate Resolution Imaging Spectroradiometer (MODIS) sensors onboard the National Aeronautics and Space Administration Terra and Aqua satellites are also popular members of the coarse-resolution group. Since becoming available in 2000, MODIS data have been extensively applied in many fields, such as land cover/land use change and atmosphere monitoring. Their ability to detect surface water has also been well demonstrated (Brakenridge & Anderson, 2006; Chen et al., 2013; Peng et al., 2005). Like other coarse spatial resolution sensors, MODIS has been widely used because of its short repeat time and broad coverage. Besides, MODIS sensors have been continuously monitoring the Earth’s surface for over a decade and have accumulated a long record that is perfect for spatio-temporal analysis of surface water dynamics. Therefore, MODIS time series data have been applied to detect lake water variations (Cai et al., 2016; Feng et al., 2012; Lu et al., 2017; Peng et al., 2005) and floodplain inundation (Huang, Chen, & Wu, 2014a; Islam et al., 2010; Ordoyne & Friedl, 2008; Yan et al., 2010) over many years.

The Visible Infrared Imaging Radiometer Suite onboard Suomi National Polar-orbiting Partnership (Suomi NPP-VIIRS) launched in 2011 is considered to be the upgrade and replacement of AVHRR and MODIS as a wide-swath multispectral sensor (Yu et al., 2005). It provides a series of multispectral bands with spatial resolutions ranging from 375 to 1,000 m. Its capability in detecting surface water has been tested (Huang et al., 2015). It has also been used for flood detection (Plumb, 2015) and shown its potential for near-real-time flood monitoring due to its high temporal resolution (Li et al., 2018). More applications of Suomi NPP-VIIRS in this field will surely emerge as time goes by and its time series grow.

The European Space Agency has also been active in monitoring ocean and land surface using optical sensors. MEdium Resolution Imaging Spectrometer (MERIS) onboard the Envisat platform, for example, has collected

300 m resolution multispectral data from 2002 to 2012. Its data have been used successfully for water/flood detection (Andreoli et al., 2007). As a follow-on of MERIS, Ocean and Land Color Instrument (OLCI) on board Sentinel-3A, which was launched in 2016, provides 21 visible and infrared bands at 300 m resolution. It will provide global coverage every two days after the launch of Sentinel-3B. We anticipate that studies using these data for water detection will appear in the literature in the near future.

2.2. Medium Spatial Resolution Sensors

Landsat is one of the most successful satellite series in history. Since the first mission was launched in 1972, it has been continuously supplying medium-resolution images for over 40 years. The sensors that were onboard early Landsat missions are Multispectral Scanner (MSS), and later upgraded to Thematic Mapper (TM) on Landsat-4 and Landsat-5, and Enhanced Thematic Mapper Plus (ETM+) on Landsat-7. Operational Land Imager (OLI) is the latest optical sensor onboard Landsat-8. The spatial resolutions of these sensors have been gradually improved from 80 to 30 m (with a 15 m resolution panchromatic band). Resolutions at this level are ideal for detecting dynamics of almost all kinds of surface water bodies. Pioneer studies were conducted in the United States, most of them mapping flood inundation extent along the Mississippi River (Deutsch & Ruggles, 1974; McGinnis & Rango, 1975). Landsat-5 had served an unexpectedly long period, which makes applications of Landsat TM images in surface water detection very common (Chen et al., 2014; Frazier et al., 2003; Frazier & Page, 2000; Pardo-Pascual et al., 2012). Launched in 2013, Landsat-8 is the most recent Landsat satellite, but its OLI data have already been widely used in detecting surface water (Acharya et al., 2016; Du et al., 2014; Gao et al., 2016; Ji et al., 2015; Li et al., 2016; Liu et al., 2016; Singh et al., 2016; Xie et al., 2016; Yang et al., 2015).

Système Probatoire d'Observation de la Terre (SPOT) is another satellite series that loaded sensors with resolutions around 10 m, which is higher than that of Landsat imagery. However, the fact that it is not freely distributed (like Landsat data) has limited its application. Nevertheless, quite a few studies have used SPOT images to detect surface water or flood inundation (Blasco et al., 1992; Davranche et al., 2010; Fisher & Danaher, 2013). Other medium-resolution sensors, such as HJ-1A/B (Lu et al., 2011) and Advanced Spaceborne Thermal Emission and Reflection Radiometer (ASTER; Sivanpillai & Miller, 2010), have also been proved effective in detecting surface water bodies.

Another satellite mission that needs to be mentioned is Sentinel-2. It is a land monitoring constellation of two satellites that provides high-resolution optical imagery for the continuity of current SPOT and Landsat missions. The Sentinel-2 mission is designed to make a global coverage of the Earth's land surface every 10 days with one satellite and 5 days with two satellites. The MultiSpectral Instrument (MSI) onboard Sentinel-2 is able to provide high-quality multispectral images with spatial resolutions ranging from 10 to 60 m. Du et al. (2016) and Yang et al. (2017) have recently verified its ability to map surface water.

2.3. High Spatial Resolution Sensors

Increasing the spatial resolution of sensors has been a key goal of remote sensing research, and significant advances have been made in the last decade. Many of the new sensors, for example, IKONOS, RapidEye, Worldview, ZY-3, Quickbird, and GF-1/2, are able to provide images with spatial resolutions at meter or even submeter level. At this level of resolutions, small water bodies can be detected successfully. But these sensors have several limitations. One is their small scene coverage, making them unsuitable for mapping large water bodies. Another is the presence of shadows on their images (Sawaya et al., 2003), especially in urban areas or mountainous regions, which can seriously affect water detection. In addition, the revisit frequency for most of these sensors, and the availability of most of their images, is also largely limited.

Despite these limitations, applications using high-resolution images to detect surface water are quite extensive. Yao et al. (2015) used ZY-3 multispectral images to detect urban surface water with high accuracy (Kappa coefficient = 0.95). Similar applications have been conducted by Xu et al. (2004) using QuickBird data, Sidle et al. (2007) using IKONOS imagery, Klemenjak et al. (2012) using RapidEye data, Zhang et al. (2014) using GF-1 data, and Xie et al. (2016) and Malinowski et al. (2015) using Worldview-2 imagery.

Some of the aforementioned sensors that have been widely used for surface water detection are listed in Table 1 for quick reference. In summary, most optical sensors can be and have been used to detect surface water. Spatial resolution is an important factor to be considered when serving this purpose. Higher spatial resolution sensors are generally able to detect surface water with a higher accuracy, but their temporal

Table 1Commonly Used Spaceborne Remote Sensors for Surface Water Detection Listed by Group^a

Sensor group	Satellite/sensor	Number of bands	Spatial resolution (m)	Temporal resolution (day)	Maximum swath at nadir (km)	Scale of application ^b	Data distribution policy (costs)	Data availability
Coarse resolution sensor	NOAA/AVHRR	5	1,100	0.5	2,800	R-G	no	1978--
	MODIS	36	250–1,000	0.5	2,330	R-G	no	1999--
	Suomi NPP-VIIRS	22	375–750	0.5	3,040	R-G	no	2012--
	MERIS	15	300	3	1,150	R-G	no	2002–2012
	Sentinel-3 OLCI	21	300	2	1,270	R-G	no	2016--
Medium resolution sensor	Landsat	4–9	15–80	16	185	L-G	no	1972--
	SPOT	4–5	2.5–20	26	120	L-R	yes	1986--
	Aster	14	15–90	16	60	L-G	no	1999--
	Sentinel-2 MSI	13	10–60	5	290	L-R	no	2015--
High resolution sensor	IKONOS	5	1–4	1.5–3	11.3	L-R	yes	1999--
	QuickBird	5	0.61–2.24	2.7	16.5	L	yes	2001--
	WorldView	4–17	0.31–2.40	1–4	17.6	L	yes	2007--
	RapidEye	5	5	1–5.5	77	L-R	yes	2008--
	ZY-3	4	2.1–5.8	5	50	L-R	yes	2012--
	GF-1/GF-2	5	1–16	4–5	800	L-R	yes	2013--

^aThe spatial resolution, temporal resolution, and spectral resolution (number of bands) vary among sensors. The area coverage (swath) determines the scale of application and also varies among sensors. ^bL, landscape; R, regional; G, global; L-R, landscape to regional; L-G, landscape to global; R-G, regional to global.

resolution is usually lower, which hampers the intensive temporal monitoring. For those extremely high resolution images such as GF-1, shadow problem and computation issue are two major defects. Besides, these data are usually not freely available. Therefore, high resolution is not always good for all situations. It is critical to choose remote sensing data with appropriate resolutions considering the scale of water bodies that are to be detected.

It should also be noted that in recent years, the successful launch of small satellite missions, particularly nanosatellites or CubeSat, has demonstrated the utility of small satellite constellations in Earth observation applications. This has resulted in the generation of larger constellations of smaller satellites, such as the Planet Labs and Skybox Imaging Earth observation constellations. They are able to achieve great temporal resolution of data and also possess very high spatial resolution. For example, with more than 170 satellites on orbit at present, the Planet constellation scans the Earth every single day, imaging the entirety of Earth's landmass at 3–5 m resolution. It is thus now possible for intensive and high-resolution monitoring of surface water or floods for specific areas, even for Arctic or sub-Arctic areas (Cooley et al., 2017).

3. Extraction of Surface Water Using Different Methods

The principle of extracting surface water from optical images is the obviously lower reflectance of water, compared to that of other land cover types, in infrared channels (Figure 3). Based on this, many methods have been developed for extracting water areas from optical remote sensing imagery. A simple method is to density slice a single infrared band to derive a water map (Frazier & Page, 2000). Either supervised or unsupervised classification methods (Manavalan et al., 1993; Ozesmi & Bauer, 2002) were used to generate land cover maps, from which water maps could be extracted. Decision trees were also built using multispectral bands to delineate water coverage from others (Acharya et al., 2016; Olthof, 2017; Sun et al., 2011). However, the problem with this kind of methods is that their classification rules are difficult to build and sometimes not robust enough to be universally applicable.

An easy and effective way to extract water is to use water indices, which are calculated from two or more bands, to identify the differences between water and nonwater areas. Many indices have been developed to extract surface water areas or flood inundation extent. For example, Crist (1985) proposed the Tasseled Cap Wetness (TCW) index derived from six bands of surface reflectance data and set a threshold of 0 to separate water and nonwater objects. Normalized difference vegetation index (NDVI), which is actually a vegetation index, has been used to detect water and flood in some studies (e.g., Domenikiotis et al., 2003). It infers the presence of water through detection of above-ground biomass but does not directly provide information

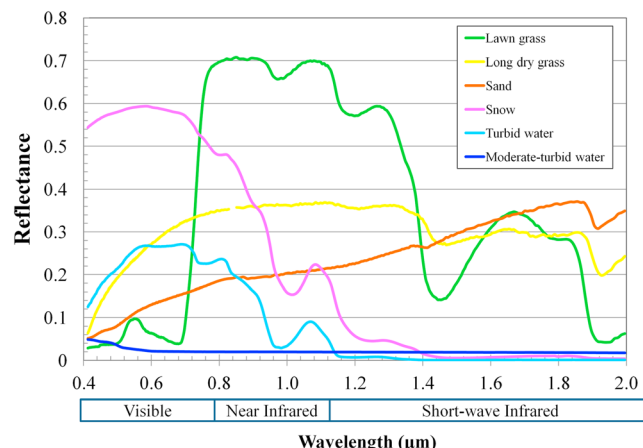


Figure 3. Reflectance of several typical land cover objects, collected from United States Geological Survey (USGS) digital spectral library (<https://speclab.cr.usgs.gov/spectral-lib.html>).

Figure 3), the normalized difference between Green band and SWIR band for snow is as high as that of water. This is why many studies (e.g., Choi & Bindschadler, 2004; Salomonson & Appel, 2004) used the normalized difference snow index (NDSI), which has an identical formula to mNDWI, to extract snow cover. This implies that caution is required when using mNDWI to extract water bodies in snow cover areas. Actually, snow can be easily distinguished from water using a single visible or NIR band, which suggests that a combination usage of mNDWI and a visible or NIR band should be able to extract surface water properly in snow cover areas.

Thresholding is one of the most critical issues in using water indices to extract water bodies. Base on the reflectance characteristics of water, NDWI and mNDWI values for water are usually greater than 0. Therefore, a threshold of 0 is often applied to extract water from index images (Xu, 2006). However, it has been suggested that adjustment of the threshold value could usually achieve better extraction results (Ji et al., 2009). This is especially tricky when thresholding either a time series of images that cover the same water body or a single image that covers a group of water bodies, because automation would be impossible if manual adjustments on threshold value for each image were required. Fortunately, many studies have been devoted to working on this issue. For example, Li and Sheng (2012) developed an automated method for mapping glacier lake dynamics using NDWI based on a local adaptive thresholding scheme. This dynamic thresholding scheme was also used on mNDWI by Allen and Pavelsky (2015) to generate a land-water mask for North America.

Feyisa et al. (2014) introduced a new index called automated water extraction index (AWEI), capable of detecting water bodies from time series Landsat imagery using a single threshold. It actually includes two indices, AWEI_{nsh}, which works well when there are no shadows, and AWEI_{sh}, which further distinguishes water pixels from shadow pixels. AWEI has been adopted in many recent studies (Tulbure et al., 2016; Xie et al., 2016) for extracting water bodies from Landsat images. Fisher et al. (2016) created a new water index, WI₂₀₁₅, using the linear discriminant analysis from surface reflectance on Visible, NIR, and SWIR channels, and proved its roughly equal strength with some other prevailing water indices. Some of the aforementioned popular water indices are listed in Table 2 for quick reference.

Table 2
Several Popular Water Indices Along With Their Equations and Sources

Indices	Equation	Sources
NDWI	$NDWI = (GREEN - NIR)/(GREEN + NIR)$	McFeeters (1996)
mNDWI	$mNDWI = (GREEN - SWIR)/(GREEN + SWIR)$	Xu (2006)
AWEI	$AWEI_{nsh} = 4 \times (GREEN - SWIR1) - (0.25 \times NIR + 2.75 \times SWIR2)$ $AWEI_{sh} = BLUE + 2.5 \times GREEN - 1.5 \times (NIR + SWIR1) - 0.25 \times SWIR2$	Feyisa et al. (2014)
WI ₂₀₁₅	$1.7204 + 171 \times GREEN + 3 \times RED - 70 \times NIR - 45 \times SWIR1 - 71 \times SWIR2$	Fisher et al. (2016)

regarding open water extraction (McFeeters, 1996). More useful indices for this purpose are those that can better highlight water bodies, such as normalized difference water index (NDWI; McFeeters, 1996), and modified NDWI (mNDWI; Xu, 2006). McFeeters's NDWI can be regarded as the first generation of water index. It was widely used in the first 10 years of the 21st century (Chowdary et al., 2008; Hui et al., 2008). Later, Xu (2006) found that the Short-wave Infrared (SWIR) band is able to reflect some subtle characteristics of water, and so replaced the Near Infrared (NIR) band in NDWI with the SWIR band and proposed the mNDWI. It is now widely accepted that mNDWI is more stable and reliable than NDWI, because the SWIR band is less sensitive to concentrations of sediments and other optical active constituents within the water than the NIR band is (see Figure 3). Therefore, mNDWI has been widely used in many recent studies (Chen et al., 2014; Mohammadi et al., 2017). One limitation of mNDWI is that it cannot discriminate water and snow, because although the snow has a generally higher reflectance than the water in all the visible and infrared channels (see

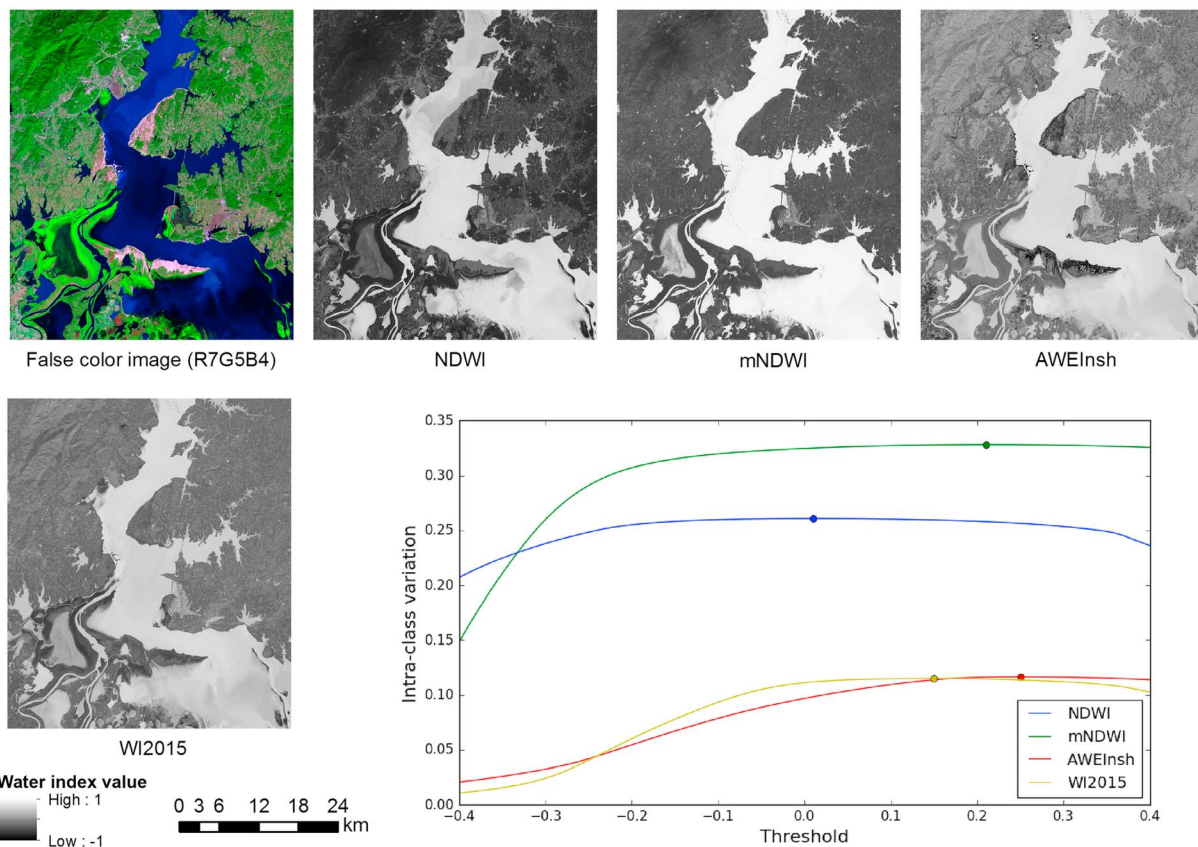


Figure 4. Landsat OLI image for Poyang Lake on 5 October 2013, corresponding images of water indices in Table 2, and line graph showing the interclass variation between water and land with different thresholds on these index images.

Basically, most indices use surface reflectance as input, considering that surface reflectance reflects the difference among land covers more accurately than other remotely sensed measurements, including digital number (DN) and top of atmosphere reflectance. However, processing remote sensing images from DN values to surface reflectance is generally time-consuming and requires a lot of computation on radiometric correction and atmospheric correction. Accurate atmospheric correction, in particular, needs some atmospheric properties, such as the aerosol concentration and optical depth, as the input information. Unfortunately, conditions and parameters of the atmosphere at the time of image acquisition are usually unknown (Du et al., 2002). Several studies tried to avoid this procedure by using DN or top of atmosphere reflectance, instead of surface reflectance, to build water indices (Danaher & Collett, 2006; Donchyts et al., 2016; Ko et al., 2015). It seems their results can be as good as those using surface reflectance in some cases (Fisher et al., 2016).

Landsat imagery is the most popular data source for calculating water indices, due to its suitable spectral bands, as well as its medium spatial resolution. We used a subset of Landsat OLI image covering Poyang Lake, China, to demonstrate the difference among those indices listed in Table 2. The false color image and corresponding index images are displayed in Figure 4 (as there was no shadow issue in this area, AWE_{Insh} was not included here). Since the original value ranges of AWE_{Insh} and WI₂₀₁₅ are not within $(-1, 1)$, we linearly stretched them to this range for a more intuitive comparison with the other indices. It is clear from Figure 4 that water bodies are easily discriminated from all of the four water index images. It is also noted that NDWI and mNDWI images have higher contrast in this case. But some water bodies may have NDWI values close to land. We examined a series of threshold values (from -0.4 to 0.4) and calculated the corresponding interclass variations between water and land (line graph in Figure 4). Higher variation means that water and land are more easily separated. The dots in the line graph represent the highest variations that were achieved with certain thresholds. In this demonstration, mNDWI performs best in delineating water from land, with a threshold value close to 0.2 making the water pixels and land pixels most separable.

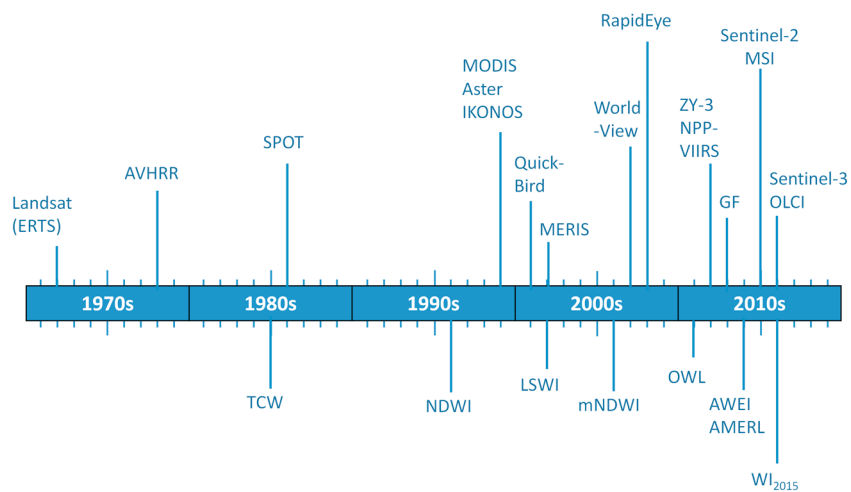


Figure 5. Timeline diagram of development of major water indices and launch of satellites/sensors.

Fisher et al. (2016) conducted a comprehensive comparison on the performance of several popular water index methods for classifying water in 30 m resolution Landsat TM/ETM+/OLI imagery. They found that the accuracy of each index was highly dependent on the composition of the validation pixels, with no index performing best across all water and nonwater pixel types. All indices and thresholds performed consistently across images from the TM, ETM +, and OLI sensors.

There were also some studies that used a combination of different indices to delineate water. Ouma and Tateishi (2006) proposed a water index that was based on a logical combination of TCW index (Crist, 1985) and NDWI for a better lake shoreline mapping. Sakamoto et al. (2007) identified flood inundation through a wavelet-based filter on the time series of land surface water index (LSWI; Xiao et al., 2002) and vegetation indices (NDVI and enhanced vegetation index) images. Lu et al. (2011) used the difference between NDVI and NDWI to differentiate water from land. Guerschman et al. (2011) proposed an Open Water Likelihood (OWL) index, which was a regression model based on five variables that are relevant to surface water, including NDVI and mNDWI. It was found that OWL is more stable over time series (Guerschman et al., 2011), which makes automatic extraction of surface water feasible through applying a single threshold for the whole time series (Huang, Chen, & Wu, 2014a). Jiang et al. (2014) proposed a water index (Automated Method for Extracting Rivers and Lakes, AMERL) that integrated NDWI, mNDWI, AWEI_{sh}, and AWEI_{nsh} to extract three water bodies in China automatically, with Kappa coefficient greater than 0.9.

Figure 5 is a timeline diagram that shows some popular water indices along with satellites/sensors. While there have been many attempts to find an automatic and universal method for extracting water area, we are yet to see methods that perform perfectly for all the sensors and all the cases. It is thus anticipated that new methods for surface water extraction will continue to emerge in the near future, with more effort likely to be put into developing highly automatic and globally applicable methods.

4. Spatio-temporal Monitoring

Surface water bodies are dynamic in nature, because they shrink or expand with time, owing to a number of natural and human-induced factors. Variations in water bodies have significant impacts on other natural resources and human assets and further influence the environment (Karpatne et al., 2016). Spatio-temporal monitoring of water body dynamics is thus essential for understanding global or regional water availability, providing descriptive insights about the natural processes that shape the storage of water resources.

Spatio-temporal monitoring of surface water dynamics is usually achieved by using multitemporal remote sensing images (Heimhuber et al., 2016; Mueller et al., 2016; Schaffer-Smith et al., 2017; Thito et al., 2016; Tulbure & Broich, 2013). One typical application is to monitor the dynamics of lake water bodies. Feng et al. (2012) used a time series of MODIS data to assess the surface water area of Poyang Lake from 2000 to 2010 and found that the lake area had been extremely variable over this period (Figure 6). Feng et al.

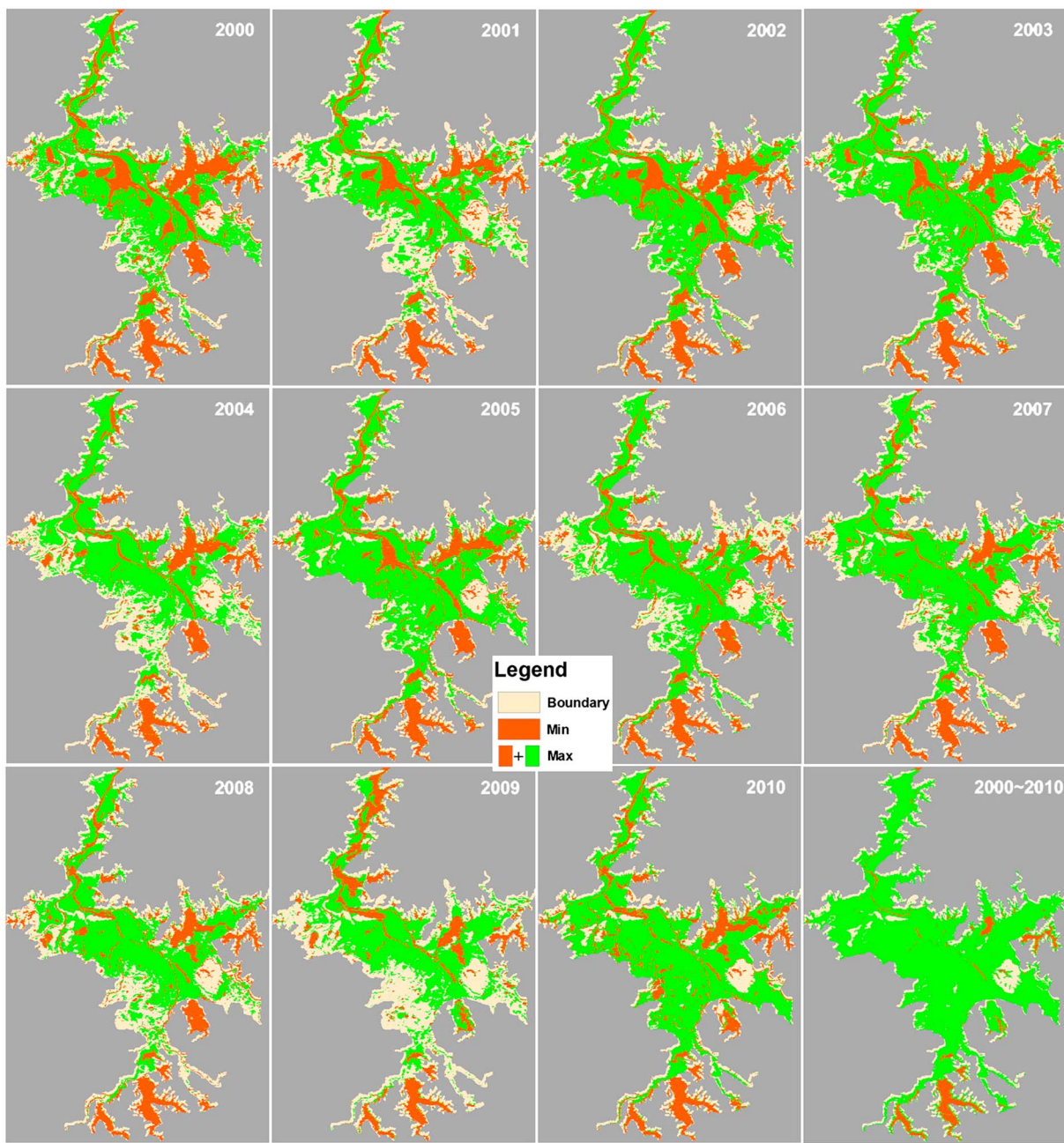


Figure 6. Minimum and maximum inundation areas and their distributions for each calendar year between 2000 and 2010. The two extreme inundation states are presented in the last panel (annotated as “2000–2010”; figure reprinted from Feng et al., 2012).

(2013) and Wu and Liu (2016) both compared the pattern of inundation dynamics in Poyang Lake and Dongting Lake using time series MODIS data. Han et al. (2015) monitored the wetland change of Poyang Lake over the last four decades using Landsat data series. Similar studies can also be found in Bai et al. (2011), Deus and Gloaguen (2013), Sheng et al. (2016), and Zhu et al. (2014). All of them demonstrated the efficiency of using optical imagery for spatio-temporal monitoring of lake water bodies.

Spatio-temporal monitoring of flood water is especially important because it is closely related to the safety of human lives and assets. Sakamoto et al. (2007) used time series MODIS imagery to investigate the temporal changes in annual flood inundation extent within the Mekong Delta. Islam et al. (2010) studied the spatial and temporal inundation variations in 2004 and 2007 in Bangladesh. Thomas et al. (2011) mapped the flood

inundation frequency in the Macquarie Marshes of Australia over 28 years using a series of Landsat images. Huang, Chen, and Wu (2014a) monitored the spatio-temporal dynamics of flood inundation over the Murray-Darling Basin of Australia using 11-year time series MODIS data. All of these studies have provided valuable information on the spatial and temporal pattern of flood inundation within different river basins.

To achieve the spatio-temporal monitoring of surface water dynamics, change detection is usually a first option. There are generally two categories of change detection methods. The first one is to classify multiple images acquired at different times and then compare the classification results (i.e., first-classify-then-compare scheme) to identify water expansion or shrinking areas. The second is to directly compare images acquired at different times, and then classify the comparison results into different change status (i.e., first-compare-then-classify scheme). First-classify-then-compare is the traditional approach and has been widely used in studies of spatio-temporal monitoring surface water (Du et al., 2012; El-Asmar & Hereher, 2011; López-Caloca et al., 2008). However, this approach usually requires enormous work in classification and accumulates a lot of errors during the comparison of classification results. Therefore, an increasing number of studies have explored methods that belong to the second category. They adopted different methods, such as image differencing (Wang, 2004; Wang et al., 2002), principal component analysis (Gianinetto et al., 2006; Rokni et al., 2014), and change vector analysis (Huang et al., 2016; Landmann et al., 2013) to first compare the original images and then identify the changed areas by classifying the comparison results. These methods reduce the amount of classification work and thus improve the efficiency of change detection.

Precise image registration is critical for successful change detection from multitemporal remotely sensed images (Sheng et al., 2008). If these images were acquired by the same satellite at the same orbit height, they are usually well matched spatially. But if they came from different sensors, careful coregistration is required to ensure that the same target is correctly represented by a single time series; otherwise, change detection might have introduced huge errors (Dai & Khorram, 1998).

5. Progresses and Challenges

5.1. Spatial and Temporal Scales

For all those sensors that are listed in section 2, there is generally a trade-off between their spatial and temporal resolutions (Huang, Chen, & Wu, 2014b). High spatial resolution sensors, such as Landsat and SPOT, usually have low temporal resolutions, generally more than 16 days, while for coarse-resolution sensors like Suomi NPP-VIIRS and MODIS, their temporal resolutions can be as fine as half a day. High temporal resolution enables intensive monitoring of surface water dynamics, while high spatial resolution ensures accurate surface water detection, yet no single remote sensing data can embrace both advantages simultaneously. However, there are two popular approaches that can alleviate this dilemma. One is pixel unmixing and reconstruction, and the other is spatial and temporal fusion.

5.1.1. Pixel Unmixing and Reconstruction

Pixel unmixing and reconstruction aim to exploit as much information as possible from a coarse pixel, and then to reconstruct it at subpixel scale. Compared to the traditional hard classification method, this approach is able to achieve higher resolution land cover mapping from coarse-resolution data under the assumption that each mixed pixel can be expressed in the form of certain combinations of a number of pure spectral signatures. It consists of two parts. The first part is to unmix coarse pixels into fractions of end-members, or so-called soft classification, or spectral mixture analysis, and the second one is to allocate subpixels according to the fraction of each end-member within each mixed coarse pixel, or so-called subpixel mapping. Figure 7 demonstrates the two procedures of pixel unmixing and reconstruction, in comparison with the traditional hard classification process. Using hard classification, the resultant map has the same spatial resolution as the original image, while using the pixel unmixing and reconstruction, a higher resolution classification map can be derived. This approach has been widely used in downscaling land cover maps (Deng & Wu, 2013; Foody & Cox, 1994; Ling et al., 2011), because it does not require additional data and is easy to implement. As a special type of land cover, surface water obviously can also be mapped using the approach of pixel unmixing and reconstruction.

The purpose of unmixing a mixed water pixel is to estimate the water fraction within it. This can be achieved by applying soft classification methods, usually based on a certain kind of spectral mixture model (Halabiský et al., 2016; Ichoku & Karnieli, 1996). The Linear Spectral Mixture Model (LSMM; Haertel & Shimabukuro, 2005)

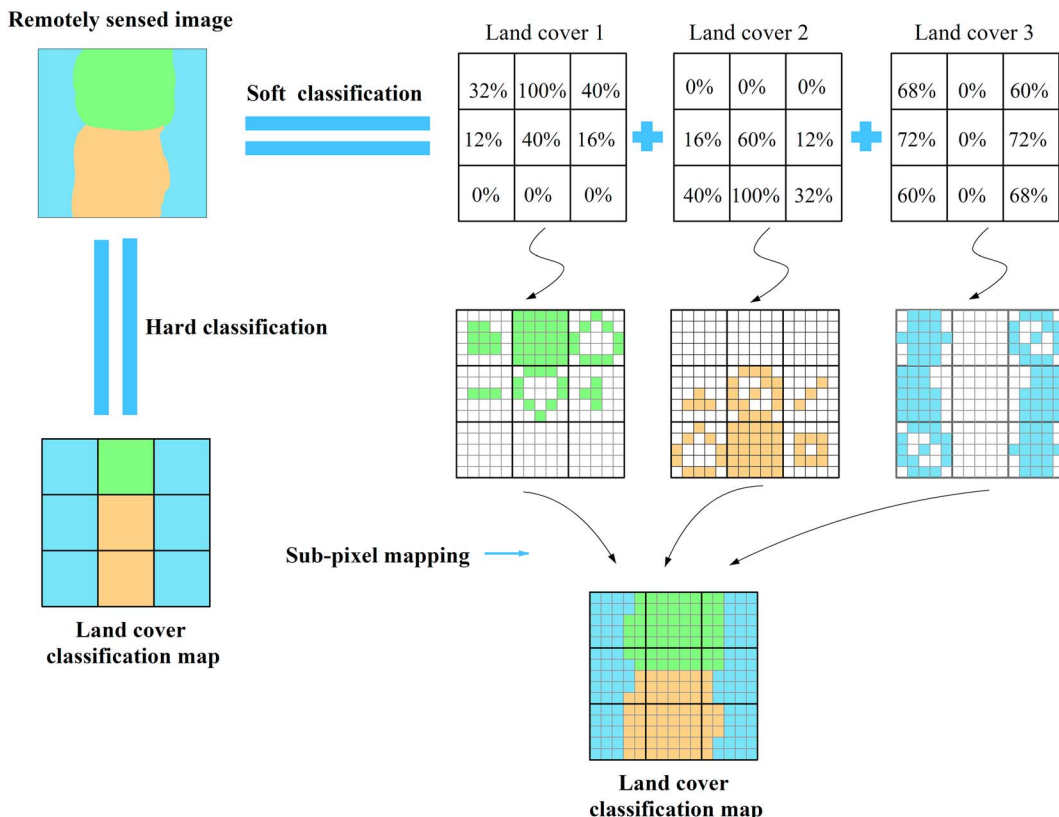


Figure 7. Demonstration of pixel unmixing and reconstruction process, in comparison with hard classification.

is among the most popular ones. Sheng et al. (2001) proposed a simple equation of estimating water fraction from NOAA/AVHRR image based on the transformation of LSMM. Li et al. (2013) introduced a dynamic nearest neighbor searching method, which is also based on LSMM, to estimate water fraction using a single MODIS SWIR band. Huang et al. (2015) presented a moving-window-based histogram method to determine endmembers for LSMM for estimating water fraction in Suomi NPP-VIIRS pixels. Except for these LSMM-based methods, there are also other methods that have been invented for this purpose, such as the multiple end-member spectral mixture analysis (Cui et al., 2011), the decision tree method (Sun et al., 2011) and the regression method (Wang et al., 2015).

The fraction map derived from the pixel unmixing approach only maintains the proportion of the same class within each pixel, without specifying the location of the class. Therefore, subpixel mapping is generally used as a follow-up procedure to produce a final subpixel scale water map. One simple and direct way of subpixel mapping is, in fact, to spatially interpolate the water fraction into the space of a coarse mixed pixel, but this usually produces a lot of speckles (Foody et al., 2005; Ling et al., 2008). Therefore, many optimization algorithms have been developed for a better subpixel mapping, such as Hopfield neural network (Tatem et al., 2002), genetic algorithm (Mertens et al., 2003), pixel swapping (Atkinson, 2005), pixel attraction model (Ling et al., 2010, 2013; Mertens et al., 2006), and particle swarm optimization (Li et al., 2015). Most of them are common subpixel mapping algorithms, which can be used for any kind of land cover. For surface water subpixel mapping in particular, there are some specific methods, such as those for lake water area mapping (Huang et al., 2017; Shah, 2011; Zhang et al., 2004), and those integrated with terrain information (Huang, Chen, & Wu, 2014b; Ling et al., 2008). All of these methods took advantage of the special characteristics of surface water, such as spatial distribution or terrain dependency, and produced better results than normal subpixel mapping algorithms.

So far, most of the aforementioned studies were concentrated on a single procedure, either pixel unmixing or subpixel mapping, because the uncertainties inevitably introduced in each procedure would be multiplied and hard to be evaluated once these two were combined. In combining these two procedures to spatially

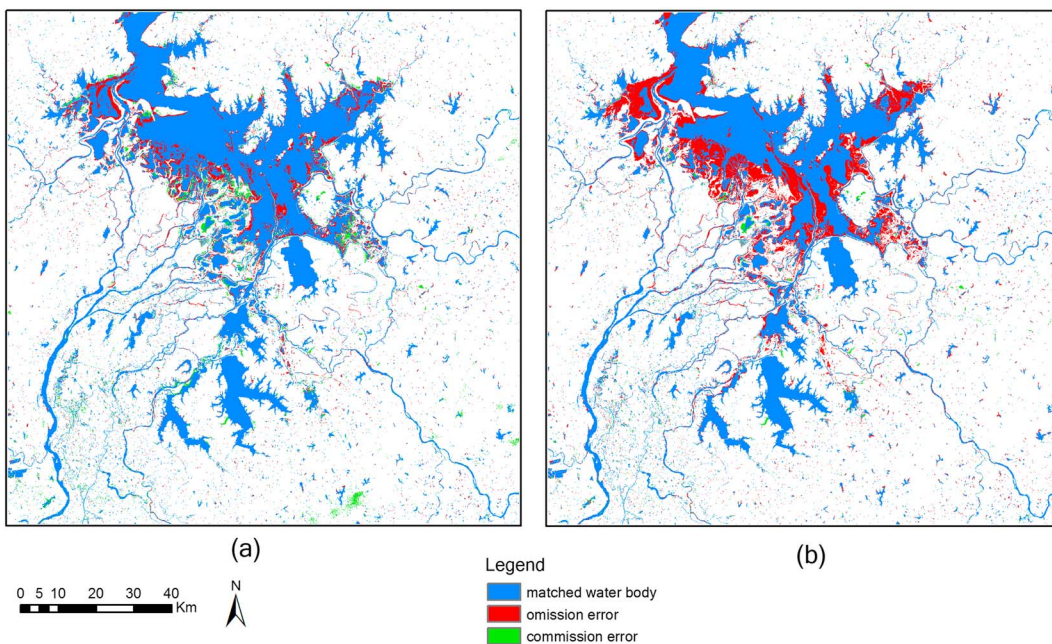


Figure 8. (a) Evaluation map of index-then-blend (IB) result. (b) Evaluation map of blend-then-index (BI) result (figure reprinted from Huang et al., 2016).

downscale lake mapping, Huang et al. (2017) found that errors and uncertainties existed in both procedures, but mainly came from the spectral unmixing procedure.

5.1.2. Spatial and Temporal Fusion

Spatial and temporal fusion (spatio-temporal fusion) is another way to deal with the trade-off between the spatial resolution and temporal resolution of remotely sensed data (Emelyanova et al., 2013). It aims to blend high spatial resolution data with high temporal resolution data to achieve both high spatial and high temporal resolutions. Several algorithms have been developed, such as the Spatial and Temporal Adaptive Reflectance Fusion Model (STARFM; Gao et al., 2006), the Enhanced STARFM (ESTARFM; Zhu et al., 2010), and the Spatio-Temporal Integrated Temperature Fusion Model (STITFM; Wu et al., 2015).

Surface water monitoring is a task that usually requires both high spatial and high temporal resolutions. Therefore, spatial and temporal fusion models should be able to improve surface water monitoring. Zhang et al. (2014) generated synthetic flooding images with improved temporal and spatial resolutions for flood mapping using both STARFM and ESTARFM and found that both models could achieve fine flood inundation monitoring results with overall accuracy around 90%.

There are usually two approaches to combine water index and spatio-temporal fusion model for producing high quality water maps (Jarihani et al., 2014). One is to first calculate a water index from multispectral data and then blend water index images using spatio-temporal fusion model (namely, index-then-blend, IB). The other is to first blend multispectral data and then calculate a water index image from the blending result (namely blend-then-index, BI). Both approaches are able to derive water index images with high spatial and high temporal resolutions, which can be easily segmented into a water map by applying an appropriate threshold. Huang et al. (2016) compared these two approaches using Poyang Lake as a case study area. Comparing with a water map derived from same-day real Landsat image, IB was superior to BI for water mapping in terms of both efficiency and accuracy (Figure 8). The overall accuracy and Kappa coefficient of IB result were 96.26% and 0.87, while those of BI result were 94.57% and 0.80. This suggests that for water monitoring purpose, we can first calculate water indices from multiple data sources and then blend the index images only. It can not only save computation time but also produce more accurate water maps.

5.2. Integration With In Situ Gauge Data

5.2.1. Combination of In Situ Gauge Data

In situ observation is one of the traditional and most reliable means of acquiring hydrological data. Gauge stations have been monitoring rivers all over the world for over a hundred years. They have collected a

long record of all kinds of hydrological data, including daily discharge and water stage, which are directly related to surface water extent and volume. However, in situ gauge data are only point-based observations. They cannot fully represent the spatial distribution of surface water. Remotely sensed data, on the other hand, provide an effective way of acquiring the spatial distribution of surface water over large areas. Frazier et al. (2003) and Frazier and Page (2009) studied the relationship between wetland inundation and river flow using Landsat data and identified a significant correlation between flow volume and remotely sensed inundation extent. Similar statistical models have been developed by empirically linking remotely sensed surface water extents to river flow or stage (Leauthaud et al., 2013; Ogilvie et al., 2015; Overton, 2005; Sagin et al., 2015; Townsend & Walsh, 1998), and all these studies have identified this correlation. This relationship could be useful for better understanding of regional or even global hydrology. For example, Pavelsky and Smith (2008b) combined in situ water level and MODIS satellite data to examine how main-stem river level fluctuations drive inundation across the Peace-Athabasca Delta, and thus help infer the hydrologic connectivity processes there.

Figure 9a shows the variation of observed flow at the upstream gauge of Narran Floodplain in Murray-Darling Basin, Australia, along with the inundation area derived from a series of MODIS images during a flood event that occurred from February to May in 2010. Synchronous and concordant variations are identified from the observed flow series and inundation area series, which suggest a close relationship between observed flow and inundation area in this area. Based on the consistency of this relationship in over 90 eco-hydrological zones (Huang et al., 2013) across the Murray-Darling Basin in Australia, Huang, Chen, and Wu (2014a) integrated time series MODIS data and a much longer time series observed flow data to model the flood inundation probability over the whole basin (Figure 9b).

Existing studies suggest that the combination of remotely sensed data with in situ data has three advantages (Huang, Chen, & Wu, 2014a). The first one is that flow data can guide image selection, especially for selecting appropriate images that captured flood events. The second advantage is that remote sensing detection can help water monitoring transfer from point-based to region-based. The third one is that the long time series of hydrological data can enrich the relatively shorter time series of remotely sensed data through modeling. For example, Heimhuber et al. (2017) built a statistical model for surface water dynamics based on a 26-year time series of Landsat-derived surface water maps in combination with river flow data from 68 gauges, and spatial time series of rainfall, evaporation, and soil moisture. Figure 10 shows the validation of modeled surface water extents (black bars) against the observed Landsat-based surface water extents (green bars) in two example floodplain modeling units (Ex-A: Lower Murray site; Ex-C: Paroo site) with contrasting flooding regimes during the 2010/2011 La Niña floods. It can be observed that the model was able to predict surface water extent with a regular interval of eight days, which is generally unachievable considering the low temporal resolution of Landsat data and occasional cloud contamination of these data. Using the observed Landsat-based surface water extents as reference, coefficients of determination (R^2) and root-mean-square error were calculated to reveal the accuracy of the modeled surface water extent. Both sites had R^2 of 0.97 and root-mean-square error less than 4%, demonstrating strong consistency between the modeled and Landsat-observed water extent.

5.2.2. Estimation of Gauge Flow Using Remote Sensing

River flow measurements are critical for water resources management, hydrological studies, and flood frequency analysis (Hirpa et al., 2013). However, the scarcity and sometime absence of observed gauge flow along river channels make the direct understanding and monitoring of surface water variation very difficult (Tarpanelli et al., 2011, 2013). Stream flow cannot be measured directly from space. Instead, satellite sensors can measure water levels, channel width, channel slope, and flow velocity. Models or statistical relationships between these variables can then be used to estimate channel flows. Therefore, remotely sensed data have been showing great potential for estimating river discharge where in situ data are difficult to obtain (Bjerkli et al., 2003).

Most remote sensing-based discharge estimation methods are based on establishing empirical rating curves that relate occasional measurements of true river discharge to another variable such as water level or inundation area that can be monitored more easily by satellites (Smith & Pavelsky, 2008). A common approach is to simply correlate remotely sensed water levels or inundation areas acquired at or near a gauging station with simultaneously collected ground data (e.g., Brakenridge et al., 2007; Pavelsky, 2014; Smith et al., 1995;

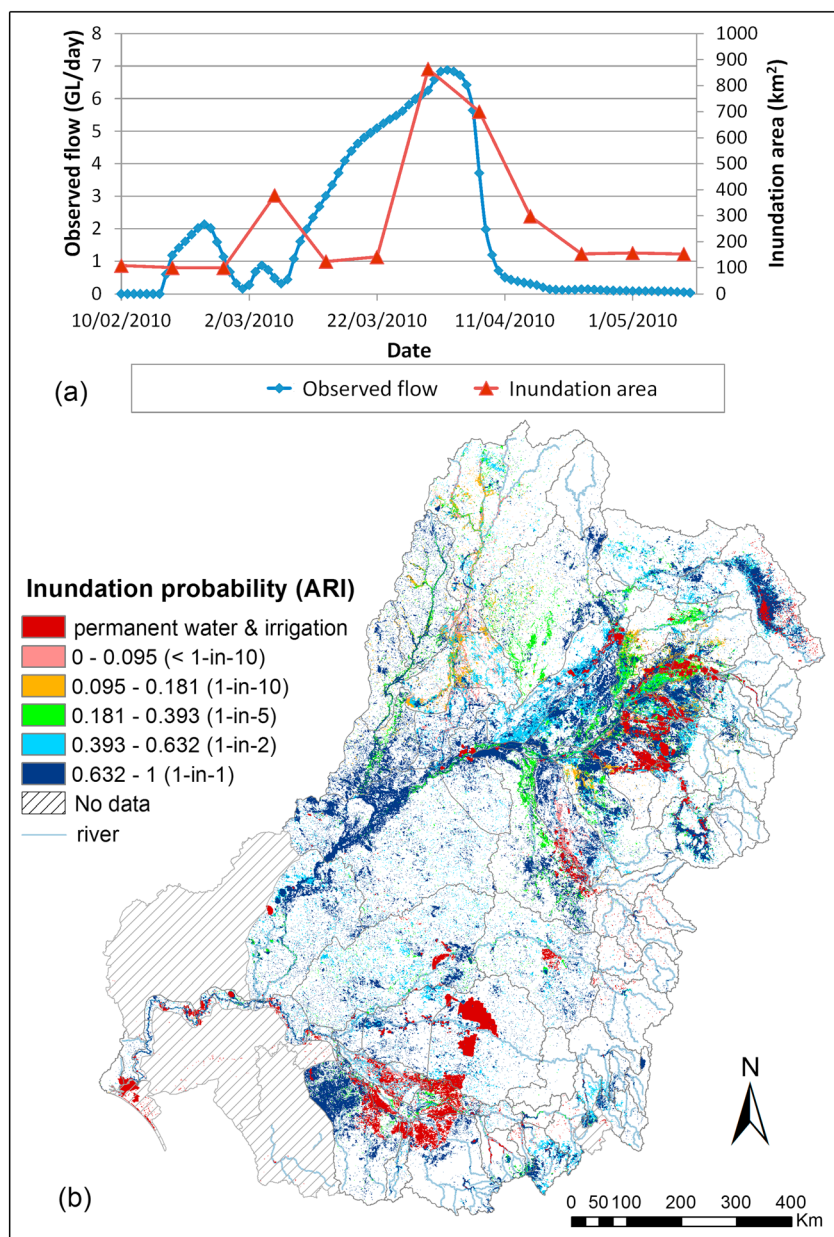


Figure 9. (a) Observed flow at the upstream gauge and inundation area derived from time series MODIS images during a flood event in Narran floodplain in the Murray-Darling Basin (MDB), Australia. (b) Modeled flood inundation probability of Annual Return Interval (ARI) for MDB based on time series MODIS data and time series observed flow data. (Figure 9b adapted from Huang, Chen, & Wu, 2014a)

Smith et al., 1996). River discharge could also be estimated by merging satellite data with topographic information into hydraulic models (e.g., Bjerklie et al., 2005; Brakenridge et al., 1998; LeFavour & Alsdorf, 2005). Satellite altimetry was also employed to assist three-dimensional remote sensing of water volume change (Alsdorf, 2003; Alsdorf et al., 2001; Frappart et al., 2005, 2006), which equates with river discharge variation. It is noted that most of the aforementioned studies used SAR data and required ancillary ground-based information such as gauge measurements, bathymetric surveys, and/or calibrated hydrology/hydraulic models. This is because the rating curves are site specific and are usually not applicable elsewhere along the same river or to other rivers of similar form (Bjerklie et al., 2003). This site-specificity greatly increases the cost of ground-based river gauging and hinders the feasibility of tracking river discharge globally (Smith & Pavelsky, 2008).

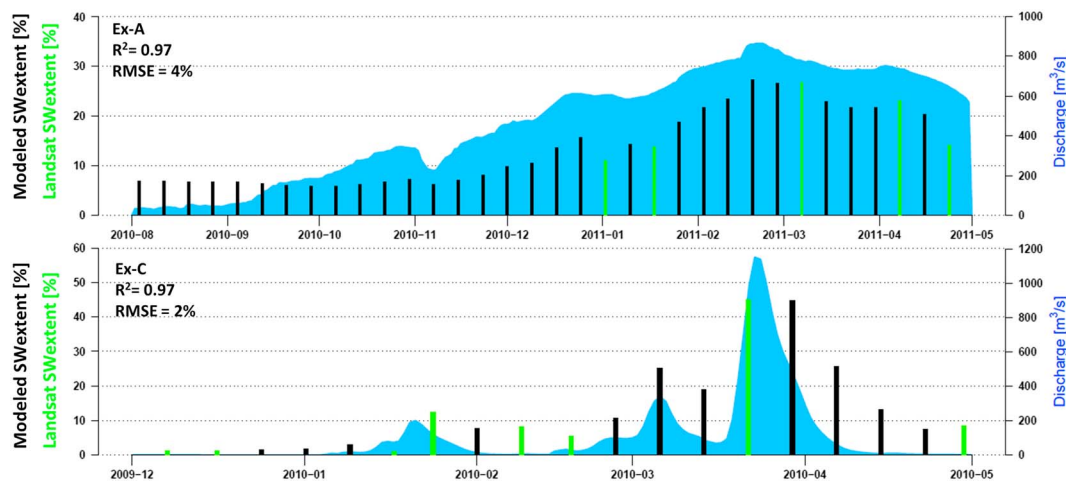


Figure 10. Comparison of the ability of statistical inundation models for quantifying surface water (SW) extent dynamics during the 2010/2011 La Niña floods based on two example floodplain modeling units (Ex-A: Lower Murray site; Ex-C: Paroo site) with contrasting flooding regimes. Shown are the hydrograph of the modeling gauge along with observed (green bars) and statistically modeled (black bars) SW extent. (figure reprinted from Heimhuber et al., 2017).

A possible limitation of using water surface area for estimation of discharge is the relatively small spatial scale of river width and associated reach surface water area changes (Bjerkle et al., 2003). Significant in-channel discharge variations along some rivers may produce river width changes of only a few meters. However, measurement locations can be increased to maximize measurement sensitivity and reliability. When water area changes over kilometers of a river reach are measured, instead of at-a-section width, then the observational precision requirements can be met (Brakenridge et al., 2007). Based on a similar consideration, Gleason and Smith (2014) found that the coefficient and exponent in at-a-station hydraulic geometry relationships are highly correlated in space, which enables the unknown parameters of these relationships to be reduced from 2 to 1. With the assistance of a genetic algorithm, they established a characteristic scaling law called a river's at-many-station hydraulic geometry, which has been explained in Gleason and Wang (2015) in details. At-many-station hydraulic geometry relationships enable river discharge to be estimated solely from river width, which can be automatically derived and easily monitored from satellite images (Isikdogan et al., 2017; Pavelsky & Smith, 2008a). Gleason et al. (2014) followed the work of Gleason and Smith (2014) with an updated methodology and a thorough sensitivity analysis of 34 rivers worldwide and found continued satisfactory performance for most river morphologies. This makes automatic discharge estimation for many large, single-thread rivers all over the world using massive archived remote sensing imagery feasible.

Brakenridge et al. (2005) and Brakenridge and Anderson (2006) found strong correlations between river discharge and MODIS band 2 (NIR band) radiance ratio, suggesting another cost-effective approach for discharge estimation. Brakenridge et al. (2007) later expanded this idea to microwave remote sensing, using the ratio between the brightness temperature measured for a pixel unaffected by the river and a pixel centered over the river itself to estimate river discharge. They used Advanced Microwave Scanning Radiometer for the Earth Observing System (AMSR-E) data to infer river discharge globally. This work has been implemented world-wide as the "Global Flood Detection System" (<http://www.gdacs.org/flooddetection/overview.aspx>) for more than 10,000 monitoring sites to serve the purposes of flood detection and also discharge estimation for ungauged and inaccessible rivers. Adopting Brakenridge et al.'s (2005) methodology, Tarpanelli et al. (2013) used four gauge stations of Po River in northern Italy as their case study and carefully selected two pixels from a MODIS NIR reflectance image. One (denoted as C) was a land pixel located near the river in an area free of surface water even during high flooding. The other one (denoted as M) was a water pixel located within the river with permanent presence of water. Their ratio (C/M) with an exponential smoothing filter applied to reduce the noise effects caused by the atmosphere (obtaining C/M*) was employed as a sensitive and consistent measurement of surface water. A strong relationship between observed flow velocity and C/M* was identified, as shown in Figure 11, demonstrating the feasibility of this method for discharge estimations. This method has also been applied to estimate discharge in the Niger-Benue River and compared with that estimated using altimetry data (Tarpanelli et al., 2017). Although

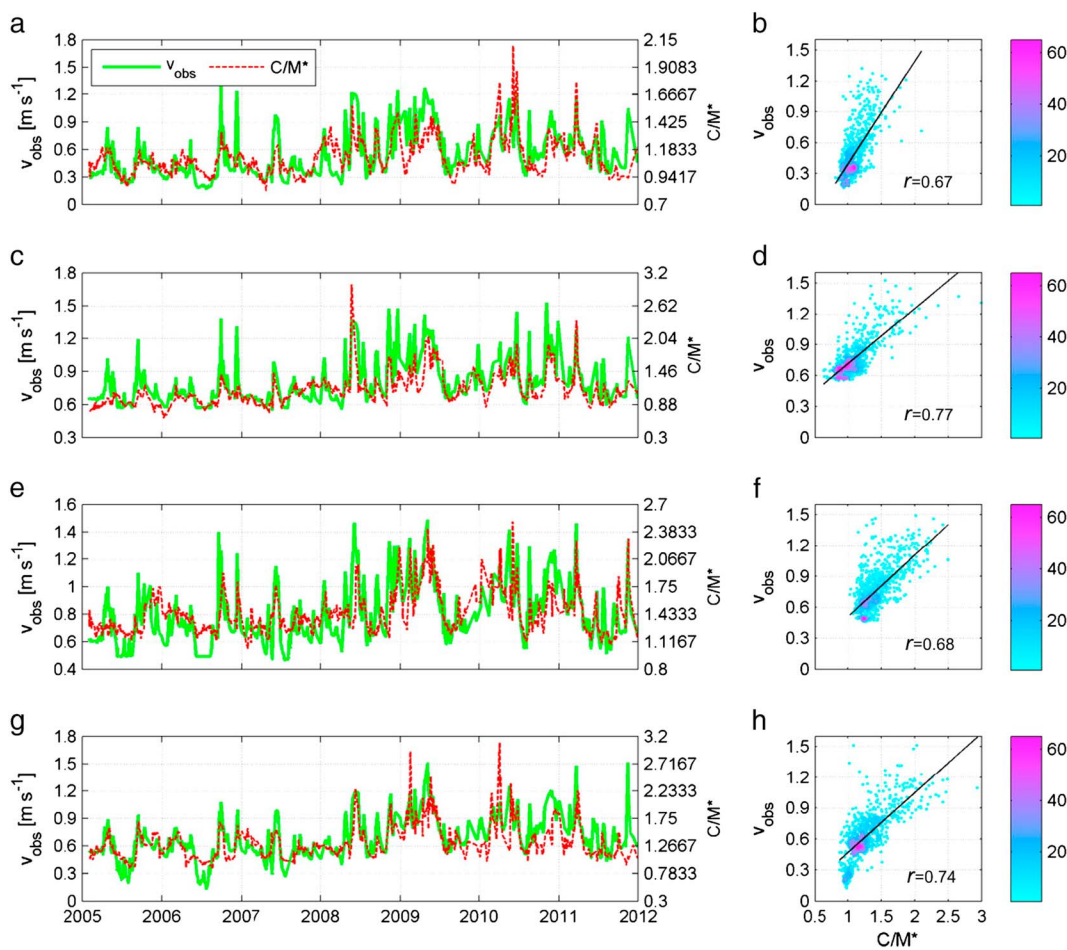


Figure 11. (left) Temporal pattern and (right) scatter plot with coefficient of correlation (r) of “observed” mean flow velocity (v_{obs}) versus the filtered C/M time series (C/M^*), for the four investigated sites: (a and b) Piacenza, (c and d) Cremona, (e and f) Borgoforte, and (g and h) Pontelagoscuro (figure reprinted from Tarpanelli et al., 2013).

altimetry was found to be more accurate in the forecasting of river discharge, the capability of MODIS data was also confirmed with performance indices >0.97 and 0.95 in terms of coefficient of correlation and Nash Sutcliffe efficiency (Nash & Sutcliffe, 1970).

Due to the high temporal variability of discharge in most rivers, remotely sensed data with high temporal resolutions, such as MODIS, are more often applied for this purpose (e.g., Tarpanelli et al., 2013). Sometimes, when high temporality is not required, higher spatial resolution data, such as Landsat (Gleason & Smith, 2014), RapidEye (Pavelsky, 2014), and QuickBird (Xu et al., 2004), can be used to estimate river discharge with high accuracy. Besides, optical sensors usually suffer from cloud cover, especially during the flood event, which hampers the correct estimation of some critical discharge records. Therefore, multisatellite techniques (Papa et al., 2008; Sichangi et al., 2016) were suggested to avoid this problem.

5.3. Terrain Dependency

The movement of surface water has a close relation with terrain, because water always flows from higher places to the connected lower places. Therefore, when studying the spatial and temporal patterns of surface water, terrain is always important supplementary information. Simple models can be established based on remotely sensed water extent and high-resolution digital elevation models (DEMs), such as light detection and ranging DEM, to simulate historical inundation changes (Huang, Peng, et al., 2014).

Water depth information is generally retrieved by coupling remote sensing imagery with ground measurements through analytical, semianalytical, or empirical modeling (Fonstad & Marcus, 2005; Gao, 2009; Legleiter et al., 2009), under the principle that the total amount of radiative energy reflected from a water

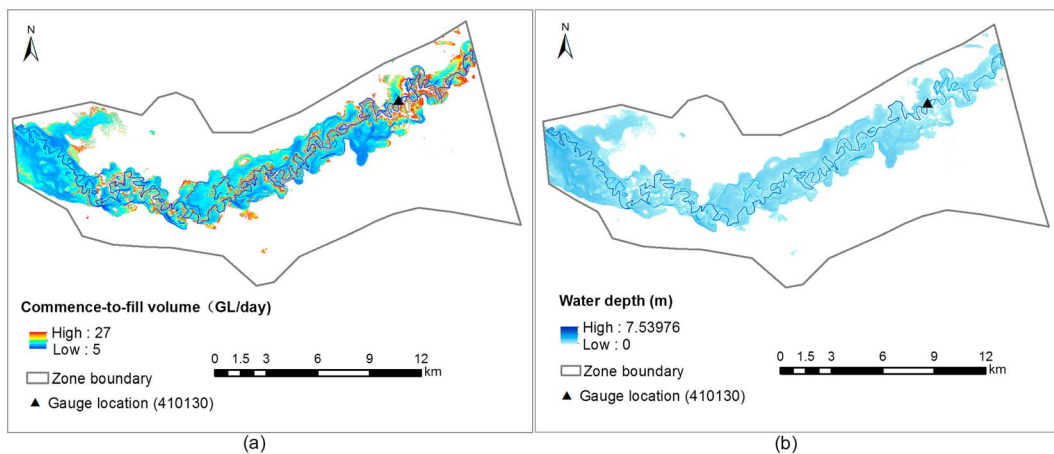


Figure 12. In a section of floodplain in the Lower Murrumbidgee River in the Murray-Darling Basin, Australia: (a) modeled commence-to-fill volumes and (b) modeled water depth under the scenario that the observed gauge flow is 26 GL/day. (figure reproduced from the published data set of Sims et al., 2014)

column is a function of water depth. Although Legleiter (2015) developed a novel framework for Flow REsistance Equation-Based Imaging of River Depths (FREEBIRD) that enabled remote sensing of river bathymetry without field measurement, Penton and Overton (2007) proposed that a more straightforward and easy-to-implement way of deriving water depth information is to integrate remotely sensed water extent and elevation data, under the assumption that water surface is flat over a certain area. Therefore, estimating water depth is easy for calm water bodies such as lakes and ponds, only if the underwater elevation is available. For large dynamic water bodies like flooding rivers, extrapolation is needed (Huang, Chen, Wu, Chen, et al., 2014; Wang, 2002) to generate a continuous height surface for water bodies that can then be used to subtract the underwater elevation to retrieve water depth. Spatial connectivity of floodplain area to river channels can be modeled by integrating gauge data and water surface height, under the assumption that a bigger observed flow generally causes a higher water surface. Sims et al. (2014) utilized Landsat imagery, light detection and ranging DEM and observed gauge flow to model the floodplain inundation under different flow volumes for the Edward-Wakool, Lower Murrumbidgee and Lower Darling River Systems in the Murray-Darling Basin, Australia. Figure 12 is a subset of the model outputs demonstrating the commence-to-fill volumes, as well as estimated water depth when the gauge flow is 26 Giga liters per day (GL/day), for a section of floodplain in the Lower Murrumbidgee River.

Another common use of terrain information is to assist inundation detection from remote sensing. DEM can describe topography at a global scale, such as the Shuttle Radar Topography Mission (SRTM) data, making this approach globally applicable. However, it should be noted that further corrections on these elevation data, such as those introduced by Yamazaki et al. (2017), might be essential to make them accurate enough to serve the purpose. Fluet-Chouinard et al. (2015) adopted SRTM-derived HydroSHED topographic information trained on a global land cover map (GLC2000; Bartholomé & Belward, 2005) to produce an inundation probability map based only on terrain data. This map was then employed to downscale the Global Inundation Extent from Multi-satellites (GIEMS; 0.25 arc-degree resolution) into 15 arc sec resolution, by distributing the inundated area of the original coarse pixels among the finer-resolution pixels with the highest probabilities of inundation. Based on similar theories, DEM data at subpixel scale resolution have been widely used for assisting subpixel water mapping (Huang, Chen, & Wu, 2014b; Li et al., 2013; Ling et al., 2008). These studies have improved the spatial allocation of water subpixels by either ranking the elevation or employing drainage pixels derived from DEMs. Their ultimate goal is to achieve subpixel scale water mapping that is more consistent with terrain and thus more reasonable, comparing to traditional subpixel mapping algorithms that are merely based on spatial contiguity.

Inundation underneath vegetation is usually hard to detect from optical images. DEM data can help identify flooding that occurred underneath forest canopies, especially within bottomland forest and hardwood swamps (Lang & McCarty, 2009; Wang et al., 2002). Shadows, especially terrain shadows, usually have similar spectral characteristics with surface water in optical images, which makes the accurate detection of water bodies difficult. DEM data can be valuable supplementary information to eliminate the confusion caused

by shadows (Gianinetto et al., 2006; Qi et al., 2009). Terrain indices, such as Multi-resolution Valley Bottom Flatness (MrVBF; Gallant & Dowling, 2003) and Height Above Nearest Drainage (HAND; Rennó et al., 2008), were developed to identify those areas with higher probability of water presence, and have provided excellent assistance for detecting surface water from remote sensing data (Donchyts et al., 2016; Huang et al., 2017; Mueller et al., 2016). More and more DEM data sources are becoming accessible, including SRTM DEM at up to 1 arc sec resolution and TanDEM-X at 12 m resolution. High-quality global terrain data sets, such as Advanced Spaceborne Thermal Emission and Reflection Radiometer Global Digital Elevation Model (ASTER GDEM) at 30 m resolution, are now publicly available, which has greatly promoted the applications of DEM in assisting global surface water mapping.

5.4. Obscuration From Clouds and Vegetation

For optical satellites, cloud coverage is always one of the most annoying issues. It may decrease image information significantly and seriously impact on the water monitoring, as well as other Earth observation applications. Mercury et al. (2012) used a MODIS cloud mask to reveal the global cloud coverage from 2000 to 2010. They found that arid regions stand out as particularly cloudless, while tropical regions stand out as particularly cloudy. This finding is generally consistent with other studies (e.g., Gunderson & Chodas, 2011; Wylie et al., 2005). Pekel et al. (2016) also found that more cloud-free observations of Landsat imagery are available during dry seasons than wet seasons. This suggests that we should be cautious when using long-term global or regional water dynamic data sets derived from time series optical images, because cloud-free observations are generally distributed unevenly both in space and over time.

In addition to the blocking effect of clouds, cloud shadowing is another obstacle that may seriously affect water detection due to the similar spectral characteristics between shadow and flood/standing water. However, this issue is not too difficult to deal with. Sheng et al. (1998) differentiated water and floods from cloud shadows based on the knowledge that NDVI is negative for water in shadowed areas. Li et al. (2013) developed an iterative method to automatically remove cloud shadows from flood/standing water in satellite maps through combining their geometric and spectral properties, because there are strong geometric correlations between clouds and cloud shadows.

Daily image composition is a common way to generate high-quality composite products that have minimum cloud coverage, for example, MODIS 8-day and 16-day composite products. The disadvantage of these products is the sacrifice of temporal resolution, and the possibility that some rapid water dynamics may be missed (Chen et al., 2013). Another popular approach for reducing cloud obscuration is to blend optical imagery with SAR imagery, taking advantage of radar's ability to penetrate cloud cover (Ward et al., 2014). However, the complexity of SAR backscatter signal is a challenge for the fusion of optical and SAR data. A detailed review of the applications of those kinds of data fusion or image fusion to land use mapping and monitoring can be found in Joshi et al. (2016).

In floodplain and wetland areas, inundation sometimes occurs underneath vegetation. In optical imagery, the vegetation cover tends to dominate the spectral signal, which can result in flooding water underneath vegetation being neglected (Guerschman et al., 2011; Soti et al., 2009). However, together with some ancillary data such as in situ water level or DEM, flood water underneath vegetation could still be mapped using optical imagery (Jin et al., 2017; Ordoyne & Friedl, 2008). A more common approach is to combine with SAR images, utilizing their ability to penetrate vegetation cover. Many studies have used optical and radar imagery jointly to detect flooded areas (Bwangoy et al., 2010; Dronova et al., 2015; Ward et al., 2014). However, there are two issues that require special attention. One is that SAR data with different wavelengths have different success rates penetrating various types of vegetation (Whitcomb et al., 2009). Therefore, it is important to select suitable data for areas with different vegetation types. The other is that optical and radar images often cannot be obtained contemporaneously, which leads to inconsistent temporal classification of land cover (Di Vittorio & Georgakakos, 2017). Fusion results should thus be used cautiously, considering that the inconsistency might have caused uncertainties.

5.5. Global Water Mapping and Monitoring

It is difficult to assess future adequacy of freshwater resources, because of the complex and rapidly changing geography of water supply and consumption (Vörösmarty et al., 2000). Global surface water mapping is a step forward for the purpose of understanding total freshwater storage and monitoring water problems over the

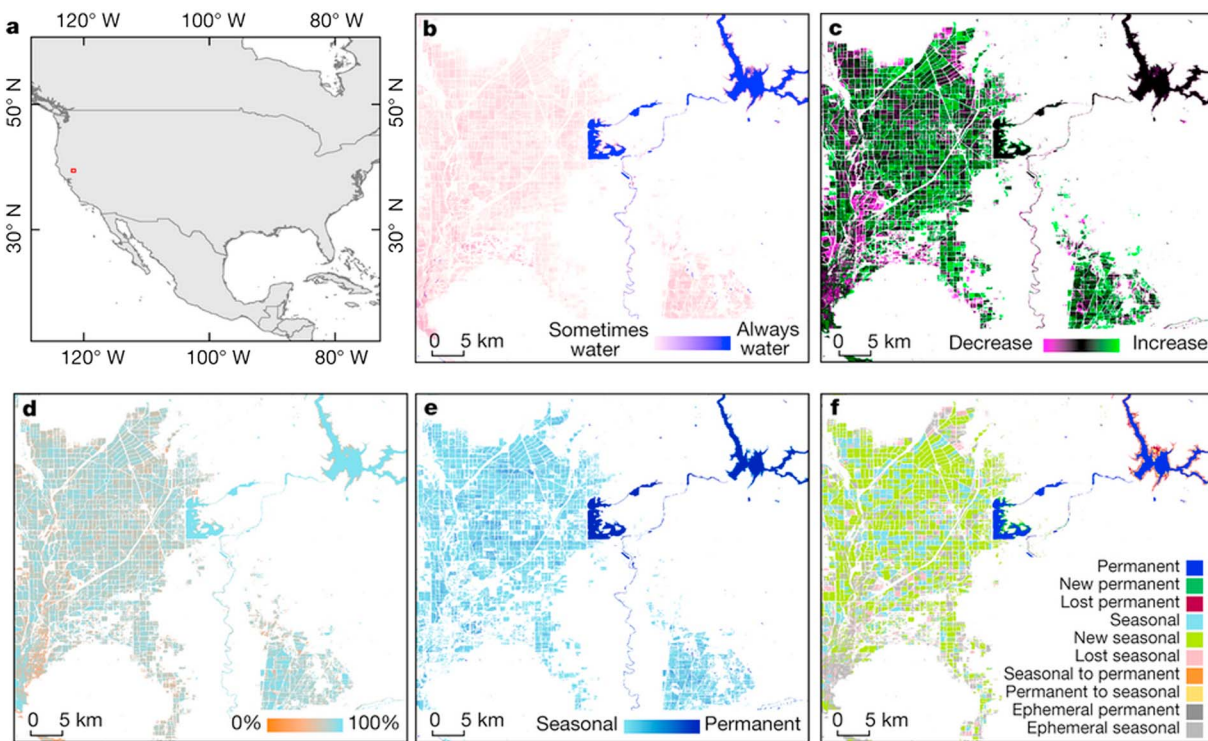


Figure 13. (a) Map of the United States showing Sacramento Valley location (red square). (b) Surface water occurrence 1984–2015. (c) Surface water occurrence change intensity 1984–2015. (d) Surface water recurrence 1984–2015. (e) Surface water seasonality 2014–2015. (f) Transitions in surface water class 1984–2015. The Sacramento Valley is one of the major rice-growing regions in the United States, extracted from the global data set. Seasonal water areas in the left and lower right of each panel correspond to flood irrigation, mainly rice paddies. The more permanent water features (middle and top right of each panel) are reservoirs (figure reprinted from Pekel et al., 2016).

world. Monitoring the dynamics of water bodies at a global scale is important for devising effective water management strategies, assessing human-induced impact on water security, understanding the interplay between global water dynamics and climate change, and mitigating disaster events, such as floods and droughts (Karpatne et al., 2016). This is why more and more attention has been paid to mapping and monitoring surface water globally, such as building an inventory of the world's lakes (Verpoorter et al., 2014).

A variety of remote sensors have been used for global water mapping and monitoring. Some studies even used a combination of multiple satellite observations to serve this purpose (Berry et al., 2005; Liao et al., 2014; Papa et al., 2010; Prigent et al., 2001, 2007). The aforementioned Global Inundation Extent from Multi-satellites (GIEMS) project (<https://lerma.obsport.fr/spip.php?article91&lang=en>; Prigent et al., 2007) combined the complementary strengths of satellite observations from the visible to the microwave to produce a low-resolution monthly data set of surface water extent and dynamics. For more detailed description about this project, the readers are referred to Prigent et al. (2016). The GIEMS database has been widely distributed and used around the world for various applications, such as estimating methane emission from wetlands (e.g., Ringeval et al., 2010; Wania et al., 2012) and hydrological modeling at continental to global scale (e.g., Decharme et al., 2008, 2012). Altimetric water levels have also been combined with the GIEMS water extent to estimate water volume changes (Frappart et al., 2008, 2010; Papa et al., 2013).

MODIS data seem to be the most popular data source for global water mapping (Carroll et al., 2009; Khandelwal et al., 2017; Sharma et al., 2015), mainly due to its high temporal resolution and sufficient spatial resolution for global scale. But as the demand for higher accuracy increases, global water maps with a higher resolution (30 m) have also been produced using Landsat data (Feng et al., 2016) and have been made freely available on the website of University of Maryland (<http://glcf.umd.edu/data/watercover/>). With the development of big data analysis and cloud platform, some new technologies, such as Google Earth Engine (GEE; Gorelick et al., 2017) and Data Cube (Lewis et al., 2017), make this task even easier. Global land and water

change over the past 30 years at 30 m resolution has also been mapped by Donchyts et al. (2016) based on GEE. A more detailed and comprehensive global surface water map (Figure 13) and its long-term change have been derived by Pekel et al. (2016) through the analysis of three million Landsat images collected over the past 32 years on the GEE platform. Their study has provided the best understanding of the changes in our planet's surface water to date (Yamazaki & Trigg, 2016). All these attempts to master global surface water dynamics will be crucial to many Earth science studies, such as climate change and global water management.

The Surface Water and Ocean Topography (SWOT) mission, planned to be launched in 2021, although not an optical sensor, is worth mentioning here. It intends to provide a major improvement in the availability of surface extent and storage change for surface water bodies such as lakes, reservoirs, wetlands, and rivers globally (Biancamaria et al., 2016). After launch, it will collect detailed measurements of how water bodies change over time on Earth (Durand et al., 2010; Lee et al., 2010), and provide novel observations for both localized studies of hydrological phenomena and improved understanding of global water cycle (Pavelsky et al., 2014). It is certain that data from SWOT could be integrated with various optical data to achieve exciting and unprecedented global water monitoring.

6. Conclusions and Outlooks

Characterization of surface water dynamics is necessary for studying ecological and hydrological processes. Remote sensing technology provides effective ways to observe surface water dynamics owing to its advantages in acquiring Earth observation information at a range of spatial, temporal, and thematic scales. This review focuses on detecting, extracting, and monitoring surface water using satellite-based optical sensors, considering those optical data that are easily available and easy to handle.

The last decade has been a golden period for optical remote sensing applications, largely due to the stable performance of MODIS and Landsat sensors, as well as the free distribution policy of their data. Similarly, some recent sensors, such as Suomi NPP-VIIRS and Sentinel-2 MSI, will surely continue to advance the field of surface water observation. In the meantime, industrial sensors with very high spatial resolution and other outstanding merits are bringing many exciting and imaginative applications to this field. Addressing the contradiction between the spatial and temporal resolutions of most satellite-based optical sensors has been a fruitful research area with methods such as pixel unmixing and reconstruction, together with spatio-temporal fusion, developed to alleviate this contradiction and achieve water monitoring with both high spatial and high temporal resolutions.

Although the principle of extracting surface water from optical sensors is straightforward, tremendous efforts have been devoted to develop automatic extraction methods. Unfortunately, a perfect method that works for all cases has not yet been developed. Contributions to the extraction methods are still expected in the near future.

We should also accept the limitations of optical remote sensing data. The most serious one is that they are easily affected by cloud obscuration. Unfortunately, clouds are almost always associated with a rainfall-induced flood event, just when inundation detection is especially valuable. Another limitation is the inability of optical sensors to see through vegetation coverage, rendering them deficient in detecting water bodies beneath vegetation. This limitation could be tackled through the assistance of terrain information. Considering the dependency between water and terrain, DEM data could also serve as ancillary information to derive water depth and to eliminate terrain shadows as well. Besides, SAR data could also be used together with optical data, because radar can penetrate the cloud and monitor the Earth's surface under all weather conditions, and even penetrate the vegetation. Fusing optical data with SAR data will certainly improve water monitoring results, bearing in mind that additional uncertainties might also be introduced by the fusion procedure.

Spatio-temporal monitoring of surface water dynamics is an essential task for many related fields, such as eco-hydrological studies and water resources management. This task usually requires skills of time series analysis or change detection on remote sensing data. It has been found that the first-compare-then-classify scheme on change detection is becoming used more widely due to its higher efficiency than the traditional first-classify-then-compare scheme.

With the increasing demand of understanding total freshwater storage and monitoring water problems over the world, global water mapping is attracting more and more attention. Multiple sources of remote sensing data with long time series and big volume have been employed to serve this purpose. Big data and cloud computation techniques have greatly promoted this field, giving birth to many exciting high-resolution and long-term global water monitoring products.

Even though the remote sensing approach is powerful in monitoring water dynamics, in situ hydrological data are still irreplaceable due to their long time series and high precision at specific locations. Taking advantage of their close relationship with remotely sensed water extent, time series flow data have been integrated with remote sensing data to build simple inundation models. Remote sensing techniques have also been applied to estimate river discharge. Recent studies have demonstrated the feasibility of using only optical remote sensing data for discharge estimation, which greatly enriches the data sources of hydrological studies, especially in those site-sparse or ungauged areas.

This review identifies the advances in water-related studies that have been achieved through applying satellite-based optical sensors, and provides sound evidence to justify ongoing investment in their use. All these applications, mentioned here or not, have greatly supported research work in many related fields, such as eco-hydrological studies and water resources management. They will provide insights into the impacts of climate change and climate oscillation on surface water distribution, and concurrently help capture human impacts on surface water resource distribution.

Acknowledgments

This work was supported by the National Key Research and Development Program of China (2017YFC0404302), National Natural Science Foundation of China (41501460 and 41671056), and China Postdoctoral Science Foundation (2016M600808). The Landsat image used for producing Figure 4 was downloaded from U.S. Geological Survey (USGS)/Earth Resources Observation and Science center (<http://eros.usgs.gov/>). All the other presented results can be found in the cited references. We would like to thank Susan Cuddy for initially reviewing this paper. We want to thank Gregory Okin, Doug Alsdorf, and three anonymous reviewers for their constructive comments.

References

- Acharya, T. D., Lee, D. H., Yang, I. T., & Lee, J. K. (2016). Identification of water bodies in a Landsat 8 OLI image using a J48 Decision Tree. *Sensors*, 16(7), 1075.
- Allen, G. H., & Pavelsky, T. M. (2015). Patterns of river width and surface area revealed by the satellite-derived North American River Width data set. *Geophysical Research Letters*, 42, 395–402. <https://doi.org/10.1002/2014GL062764>
- Alsdorf, D., Birkett, C., Dunne, T., Melack, J., & Hess, L. (2001). Water level changes in a large Amazon lake measured with spaceborne radar interferometry and altimetry. *Geophysical Research Letters*, 28(14), 2671–2674. <https://doi.org/10.1029/2001GL012962>
- Alsdorf, D. E. (2003). Water storage of the central Amazon floodplain measured with GIS and remote sensing imagery. *Annals of the Association of American Geographers*, 93(1), 55–66. <https://doi.org/10.1111/1467-8306.93105>
- Alsdorf, D. E., & Lettenmaier, D. P. (2003). Tracking fresh water from space. *Science*, 301(5639), 1491–1494.
- Alsdorf, D. E., Rodriguez, E., & Lettenmaier, D. P. (2007). Measuring surface water from space. *Reviews of Geophysics*, 45, RG2002. <https://doi.org/10.1029/2006RG000197>
- Andreoli, R., Yesou, H., Li, J., & Desnos, Y. L. (2007). *Inland lake monitoring using low and medium resolution ENVISAT ASAR and optical data: Case study of Poyang Lake (Jiangxi, P.R. China)*. Paper presented at 2007 IEEE International Geoscience and Remote Sensing Symposium, Barcelona, Spain.
- Atkinson, P. M. (2005). Sub-pixel target mapping from soft-classified, remotely sensed imagery. *Photogrammetric Engineering and Remote Sensing*, 71(7), 839–846.
- Bai, J., Chen, X., Li, J., Yang, L., & Fang, H. (2011). Changes in the area of inland lakes in arid regions of central Asia during the past 30 years. *Environmental Monitoring and Assessment*, 178(1–4), 247–256. <https://doi.org/10.1007/s10661-010-1686-y>
- Bartholomé, E., & Belward, A. (2005). GLC2000: A new approach to global land cover mapping from Earth observation data. *International Journal of Remote Sensing*, 26(9), 1959–1977.
- Barton, I. J., & Bathols, J. M. (1989). Monitoring floods with AVHRR. *Remote Sensing of Environment*, 30(1), 89–94. [https://doi.org/10.1016/0034-4257\(89\)90050-3](https://doi.org/10.1016/0034-4257(89)90050-3)
- Berry, P. A. M., Garlick, J. D., Freeman, J. A., & Mathers, E. L. (2005). Global inland water monitoring from multi-mission altimetry. *Geophysical Research Letters*, 32, L16401. <https://doi.org/10.1029/2005GL022814>
- Bhavasar, P. D. (1984). Review of remote sensing applications in hydrology and water resources management in India. *Advances in Space Research*, 4(11), 193–200. [https://doi.org/10.1016/0273-1177\(84\)90411-3](https://doi.org/10.1016/0273-1177(84)90411-3)
- Biancamaria, S., Lettenmaier, D. P., & Pavelsky, T. M. (2016). The SWOT mission and its capabilities for land hydrology. *Surveys in Geophysics*, 37(2), 307–337. <https://doi.org/10.1007/s10712-015-9346-y>
- Bjerkle, D. M., Lawrence Dingman, S., Vorusmarti, C. J., Bolster, C. H., & Congalton, R. G. (2003). Evaluating the potential for measuring river discharge from space. *Journal of Hydrology*, 278(1–4), 17–38. [https://doi.org/10.1016/S0022-1694\(03\)00129-X](https://doi.org/10.1016/S0022-1694(03)00129-X)
- Bjerkle, D. M., Moller, D., Smith, L. C., & Dingman, S. L. (2005). Estimating discharge in rivers using remotely sensed hydraulic information. *Journal of Hydrology*, 309(1), 191–209. <https://doi.org/10.1016/j.jhydrol.2004.11.022>
- Blasco, F., Bellan, M. F., & Chaudhury, M. U. (1992). Estimating the extent of floods in Bangladesh using SPOT data. *Remote Sensing of Environment*, 39(3), 167–178. [https://doi.org/10.1016/0034-4257\(92\)90083-v](https://doi.org/10.1016/0034-4257(92)90083-v)
- Brakenridge, R., & Anderson, E. (2006). Modis-based flood detection, mapping and measurement: The potential for operational hydrological applications. In J. Marsalek, G. Stancalje, & G. Balint (Eds.), *Transboundary Floods: Reducing Risks Through Flood Management* (pp. 1–12). Dordrecht, Netherlands: Springer.
- Brakenridge, G. R., Nghiem, S. V., Anderson, E., & Chien, S. (2005). Space-based measurement of river runoff. *Eos, Transactions American Geophysical Union*, 86(19). <https://doi.org/10.1029/2005EO190001>
- Brakenridge, G. R., Nghiem, S. V., Anderson, E., & Mic, R. (2007). Orbital microwave measurement of river discharge and ice status. *Water Resources Research*, 43, W04405. <https://doi.org/10.1029/2006WR005238>
- Brakenridge, G. R., Tracy, B. T., & Knox, J. C. (1998). Orbital SAR remote sensing of a river flood wave. *International Journal of Remote Sensing*, 19(7), 1439–1445. <https://doi.org/10.1080/014311698215559>

- Bwangoy, J.-R. B., Hansen, M. C., Roy, D. P., Grandi, G. D., & Justice, C. O. (2010). Wetland mapping in the Congo Basin using optical and radar remotely sensed data and derived topographical indices. *Remote Sensing of Environment*, 114(1), 73–86. <https://doi.org/10.1016/j.rse.2009.08.004>
- Cai, X., Feng, L., Hou, X., & Chen, X. (2016). Remote sensing of the water storage dynamics of large lakes and reservoirs in the Yangtze River Basin from 2000 to 2014. *Scientific Reports*, 6, 36405. <https://doi.org/10.1038/srep36405>
- Carroll, M. L., Townshend, J. R., DiMiceli, C. M., Noojipady, P., & Sohlberg, R. A. (2009). A new global raster water mask at 250 m resolution. *International Journal of Digital Earth*, 2(4), 291–308. <https://doi.org/10.1080/17538940902951401>
- Chen, Y., Huang, C., Ticehurst, C., Merrin, L., & Thew, P. (2013). An evaluation of MODIS daily and 8-day composite products for floodplain and wetland inundation mapping. *Wetlands*, 33(5), 823–835. <https://doi.org/10.1007/s13157-013-0439-4>
- Chen, Y., Wang, B., Pollino, C. A., Cuddy, S. M., Merrin, L. E., & Huang, C. (2014). Estimate of flood inundation and retention on wetlands using remote sensing and GIS. *Ecohydrology*, 7, 1412–1420. <https://doi.org/10.1002/eco.1467>
- Choi, H., & Bindschadler, R. (2004). Cloud detection in Landsat imagery of ice sheets using shadow matching technique and automatic normalized difference snow index threshold value decision. *Remote Sensing of Environment*, 91(2), 237–242. <https://doi.org/10.1016/j.rse.2004.03.007>
- Chowdary, V. M., Chandran, R. V., Neeti, N., Bothale, R. V., Srivastava, Y. K., Ingle, P., et al. (2008). Assessment of surface and sub-surface waterlogged areas in irrigation command areas of Bihar state using remote sensing and GIS. *Agricultural Water Management*, 95(7), 754–766. <https://doi.org/10.1016/j.agwat.2008.02.009>
- Cooley, S., Smith, L., Stepan, L., & Mascaro, J. (2017). Tracking dynamic northern surface water changes with high-frequency planet CubeSat imagery. *Remote Sensing*, 9(12), 1306. <https://doi.org/10.3390/rs9121306>
- Crist, E. P. (1985). A TM Tasseled Cap equivalent transformation for reflectance factor data. *Remote Sensing of Environment*, 17(3), 301–306. [https://doi.org/10.1016/0034-4257\(85\)90102-6](https://doi.org/10.1016/0034-4257(85)90102-6)
- Cui, Q., Shi, J. C., & Xu, Y. L. (2011). *Estimation of sub-pixel water area on Tibet Plateau using multiple endmembers spectral mixture spectral analysis from MODIS data*. Paper presented at 7th Symposium on Multispectral Image Processing and Pattern Recognition (MIPPR) - Remote Sensing Image Processing, Geographic Information Systems, and Other Applications, Guilin, China.
- Dai, X., & Khorram, S. (1998). The effects of image misregistration on the accuracy of remotely sensed change detection. *IEEE Transactions on Geoscience and Remote Sensing*, 36(5), 1566–1577.
- Danaher, T., & Collett, L. (2006). *Development, optimisation and multi-temporal application of a simple Landsat based water index*. Paper presented at 13th Australasian Remote Sensing and Photogrammetry Conference, Canberra, Australia.
- Davranche, A., Lefebvre, G., & Poulin, B. (2010). Wetland monitoring using classification trees and SPOT-5 seasonal time series. *Remote Sensing of Environment*, 114(3), 552–562. <https://doi.org/10.1016/j.rse.2009.10.009>
- Decharme, B., Alkama, R., Papa, F., Faroux, S., Douville, H., & Prigent, C. (2012). Global off-line evaluation of the ISBA-TRIP flood model. *Climate Dynamics*, 38, 1389–1412.
- Decharme, B., Douville, H., Prigent, C., Papa, F., & Aires, F. (2008). A new river flooding scheme for global climate applications: Off-line evaluation over South America. *Journal of Geophysical Research*, 113, D11110. <https://doi.org/10.1029/2007JD009376>
- Deng, C., & Wu, C. (2013). A spatially adaptive spectral mixture analysis for mapping subpixel urban impervious surface distribution. *Remote Sensing of Environment*, 133(0), 62–70. <https://doi.org/10.1016/j.rse.2013.02.005>
- Deus, D., & Gloaguen, R. (2013). Remote sensing analysis of lake dynamics in semi-arid regions: implication for water resource management. Lake Manyara, East African Rift, Northern Tanzania. *Water*, 5(2), 698–727.
- Deutsch, M., & Ruggles, F. (1974). Optical data processing and projected applications of the ERTS-1 imagery covering the 1973 Mississippi River Valley floods. *Water Resources Bulletin*, 10(5), 1023–1039.
- Di Vittorio, C. A., & Georgakakos, A. P. (2017). Land cover classification and wetland inundation mapping using MODIS. *Remote Sensing of Environment*, 204(1), 1–17. <https://doi.org/10.1016/j.rse.2017.11.001>
- Domenikotis, C., Loukas, A., & Dalezios, N. R. (2003). The use of NOAA/AVHRR satellite data for monitoring and assessment of forestfires and flood. *Natural Hazards and Earth System Sciences*, 3, 115–128.
- Donchyts, G., Baart, F., Winsemius, H., Gorelick, N., Kwadijk, J., & van de Giesen, N. (2016). Earth's surface water change over the past 30 years. *Nature Climate Change*, 6(9), 810–813.
- Donchyts, G., Schellekens, J., Winsemius, H., Eisemann, E., & van de Giesen, N. (2016). A 30 m resolution surface water mask including estimation of positional and thematic differences using Landsat 8, SRTM and OpenStreetMap: A case study in the Murray-Darling Basin, Australia. *Remote Sensing*, 8(5), 386.
- Dronova, I., Gong, P., Wang, L., & Zhong, L. (2015). Mapping dynamic cover types in a large seasonally flooded wetland using extended principal component analysis and object-based classification. *Remote Sensing of Environment*, 158(Supplement C), 193–206. <https://doi.org/10.1016/j.rse.2014.10.027>
- Du, Z., Li, W., Zhou, D., Tian, L., Ling, F., Wang, H., et al. (2014). Analysis of Landsat-8 OLI imagery for land surface water mapping. *Remote Sensing Letters*, 5(7), 672–681. <https://doi.org/10.1080/2150704X.2014.960606>
- Du, Z., Linghu, B., Ling, F., Li, W., Tian, W., Wang, H., et al. (2012). Estimating surface water area changes using time-series Landsat data in the Qingjiang River Basin, China. *Journal of Applied Remote Sensing*, 6(1), 063609. <https://doi.org/10.1117/1.JRS.6.063609>
- Du, Y., Teillet, P. M., & Cihlar, J. (2002). Radiometric normalization of multitemporal high-resolution satellite images with quality control for land cover change detection. *Remote Sensing of Environment*, 82(1), 123–134.
- Du, Y., Zhang, Y., Ling, F., Wang, Q., Li, W., & Li, X. (2016). Water bodies' mapping from Sentinel-2 imagery with modified normalized difference water index at 10-m spatiereolution produced by sharpening the SWIR band. *Remote Sensing*, 8(4), 354.
- Durand, M., Fu, L. L., Lettenmaier, D. P., Alsdorf, D. E., Rodriguez, E., & Esteban-Fernandez, D. (2010). The Surface Water and Ocean Topography mission: Observing terrestrial surface water and oceanic submesoscale eddies. *Proceedings of the IEEE*, 98(5), 766–779. <https://doi.org/10.1109/JPROC.2010.2043031>
- El-Asmar, H., & Hereher, M. (2011). Change detection of the coastal zone east of the Nile Delta using remote sensing. *Environment and Earth Science*, 62(4), 769–777.
- Emelyanova, I. V., McVicar, T. R., Van Niel, T. G., Li, L. T., & van Dijk, A. I. J. M. (2013). Assessing the accuracy of blending Landsat-MODIS surface reflectances in two landscapes with contrasting spatial and temporal dynamics: A framework for algorithm selection. *Remote Sensing of Environment*, 133, 193–209. <https://doi.org/10.1016/j.rse.2013.02.007>
- Feng, L., Hu, C., Chen, X., & Zhao, X. (2013). Dramatic inundation changes of China's two largest freshwater lakes linked to the Three Gorges Dam. *Environmental Science & Technology*, 47(17), 9628–9634. <https://doi.org/10.1021/es4009618>
- Feng, L., Hu, C. M., Chen, X. L., Cai, X. B., Tian, L. Q., & Gan, W. X. (2012). Assessment of inundation changes of Poyang Lake using MODIS observations between 2000 and 2010. *Remote Sensing of Environment*, 121, 80–92. <https://doi.org/10.1016/j.rse.2012.01.014>

- Feng, M., Sexton, J. O., Channan, S., & Townshend, J. R. (2016). A global, high-resolution (30-m) inland water body dataset for 2000: First results of a topographic-spectral classification algorithm. *International Journal of Digital Earth*, 9(2), 113–133. <https://doi.org/10.1080/17538947.2015.1026420>
- Feyisa, G. L., Meilby, H., Fensholt, R., & Proud, S. R. (2014). Automated water extraction index: A new technique for surface water mapping using Landsat imagery. *Remote Sensing of Environment*, 140(0), 23–35. <https://doi.org/10.1016/j.rse.2013.08.029>
- Fisher, A., & Danaher, T. (2013). A water index for SPOT5 HRG satellite imagery, New South Wales, Australia, determined by linear discriminant analysis. *Remote Sensing*, 5(11), 5907–5925.
- Fisher, A., Flood, N., & Danaher, T. (2016). Comparing Landsat water index methods for automated water classification in eastern Australia. *Remote Sensing of Environment*, 175, 167–182. <https://doi.org/10.1016/j.rse.2015.12.055>
- Fluet-Chouinard, E., Lehner, B., Rebelo, L.-M., Papa, F., & Hamilton, S. K. (2015). Development of a global inundation map at high spatial resolution from topographic downscaling of coarse-scale remote sensing data. *Remote Sensing of Environment*, 158, 348–361. <https://doi.org/10.1016/j.rse.2014.10.015>
- Fonstad, M. A., & Marcus, W. A. (2005). Remote sensing of stream depths with hydraulically assisted bathymetry (HAB) models. *Geomorphology*, 72(1), 320–339. <https://doi.org/10.1016/j.geomorph.2005.06.005>
- Foody, G. M., & Cox, D. P. (1994). Sub-pixel land cover composition estimation using a linear mixture model and fuzzy membership functions. *International Journal of Remote Sensing*, 15(3), 619–631. <https://doi.org/10.1080/01431169408954100>
- Foody, G. M., Muslim, A. M., & Atkinson, P. M. (2005). Super-resolution mapping of the waterline from remotely sensed data. *International Journal of Remote Sensing*, 26(24), 5381–5392. <https://doi.org/10.1080/01431160500213292>
- Frappart, F., Do Minh, K., L'Hermitte, J., Cazenave, A., Ramillien, G., Le Toan, T., & Mognard-Campbell, N. (2006). Water volume change in the lower Mekong from satellite altimetry and imagery data. *Geophysical Journal International*, 167(2), 570–584. <https://doi.org/10.1111/j.1365-246X.2006.03184.x>
- Frappart, F., Papa, F., Famiglietti, J. S., Prigent, C., Rossow, W. B., & Seyler, F. (2008). Interannual variations of river water storage from a multiple satellite approach: A case study for the Rio Negro River basin. *Journal of Geophysical Research*, 113, D21104. <https://doi.org/10.1029/2007JD009438>
- Frappart, F., Papa, F., Guntner, A., Werth, S., Ramillien, G., Prigent, C., et al. (2010). Interannual variations of the terrestrial water storage in the Lower Ob' Basin from a multisatellite approach. *Hydrology and Earth System Sciences*, 14(12), 2443–2453.
- Frappart, F., Seyler, F., Martinez, J.-M., León, J. G., & Cazenave, A. (2005). Floodplain water storage in the Negro River basin estimated from microwave remote sensing of inundation area and water levels. *Remote Sensing of Environment*, 99(4), 387–399. <https://doi.org/10.1016/j.rse.2005.08.016>
- Frazier, P., & Page, K. (2009). A reach-scale remote sensing technique to relate wetland inundation to river flow. *River Research and Applications*, 25(7), 836–849. <https://doi.org/10.1002/rra.1183>
- Frazier, P., Page, K., Louis, J., Briggs, S., & Robertson, A. I. (2003). Relating wetland inundation to river flow using Landsat TM data. *International Journal of Remote Sensing*, 24(19), 3755–3770. <https://doi.org/10.1080/0143116021000023916>
- Frazier, P. S., & Page, K. J. (2000). Water body detection and delineation with Landsat TM data. *Photogrammetric Engineering and Remote Sensing*, 66(12), 1461–1467.
- Gallant, J. C., & Dowling, T. I. (2003). A multiresolution index of valley bottom flatness for mapping depositional areas. *Water Resources Research*, 39(12), 1347. <https://doi.org/10.1029/2002WR001426>
- Gao, F., Masek, J., Schwaller, M., & Hall, F. (2006). On the blending of the Landsat and MODIS surface reflectance: Predicting daily Landsat surface reflectance. *IEEE Transactions on Geoscience and Remote Sensing*, 44(8), 2207–2218. <https://doi.org/10.1109/tgrs.2006.872081>
- Gao, H., Wang, L., Jing, L., & Xu, J. (2016). An effective modified water extraction method for Landsat-8 OLI imagery of mountainous plateau regions. Paper presented at IOP Conference Series: Earth and Environmental Science, Beijing, China.
- Gao, J. (2009). Bathymetric mapping by means of remote sensing: methods, accuracy and limitations. *Progress in Physical Geography*, 33(1), 103–116. <https://doi.org/10.1177/030913309105657>
- Gianinetto, M., Villa, P., & Lechi, G. (2006). Postflood damage evaluation using landsat TM and ETM plus data integrated with DEM. *IEEE Transactions on Geoscience and Remote Sensing*, 44(1), 236–243. <https://doi.org/10.1109/tgrs.2005.859952>
- Gleason, C. J., & Smith, L. C. (2014). Toward global mapping of river discharge using satellite images and at-many-stations hydraulic geometry. *Proceedings of the National Academy of Sciences of the United States of America*, 111(13), 4788–4791. <https://doi.org/10.1073/pnas.1317606111>
- Gleason, C. J., Smith, L. C., & Lee, J. (2014). Retrieval of river discharge solely from satellite imagery and at-many-stations hydraulic geometry: Sensitivity to river form and optimization parameters. *Water Resources Research*, 50, 9604–9619. <https://doi.org/10.1002/2014WR016109>
- Gleason, C. J., & Wang, J. (2015). Theoretical basis for at-many-stations hydraulic geometry. *Geophysical Research Letters*, 42, 7107–7114. <https://doi.org/10.1002/2015GL064935>
- Gorelick, N., Hancher, M., Dixon, M., Ilyushchenko, S., Thau, D., & Moore, R. (2017). Google Earth Engine: Planetary-scale geospatial analysis for everyone. *Remote Sensing of Environment*, 202(Supplement C), 18–27. <https://doi.org/10.1016/j.rse.2017.06.031>
- Guerszman, J. P., Warren, G., Byrne, G., Lymburner, L., Mueller, N., & Van Dijk, A. (2011). MODIS-based standing water detection for flood and large reservoir mapping: algorithm development and applications for the Australian continent. In *CSIRO: Water for a Healthy Country National Research Flagship Report* (p. 100). Canberra, Australia: CSIRO.
- Gunderson, A., & Chodas, M. (2011). An investigation of cloud cover probability for the HypsIIRI mission using MODIS cloud mask data. Paper presented at 2011 IEEE Aerospace Conference, Big Sky, MT, USA
- Haertel, V. F., & Shimabukuro, Y. E. (2005). Spectral linear mixing model in low spatial resolution image data. *IEEE Transactions on Geoscience and Remote Sensing*, 43(11), 2555–2562. <https://doi.org/10.1109/tgrs.2005.848692>
- Halabisky, M., Moskal, L. M., Gillespie, A., & Hannam, M. (2016). Reconstructing semi-arid wetland surface water dynamics through spectral mixture analysis of a time series of Landsat satellite images (1984–2011). *Remote Sensing of Environment*, 177, 171–183. <https://doi.org/10.1016/j.rse.2016.02.040>
- Han, X., Chen, X., & Feng, L. (2015). Four decades of winter wetland changes in Poyang Lake based on Landsat observations between 1973 and 2013. *Remote Sensing of Environment*, 156, 426–437.
- Heimhuber, V., Tulbure, M. G., & Broich, M. (2016). Modeling 25 years of spatio-temporal surface water and inundation dynamics on large river basin scale using time series of Earth observation data. *Hydrology and Earth System Sciences*, 20(6), 2227–2250. <https://doi.org/10.5194/hess-20-2227-2016>
- Heimhuber, V., Tulbure, M. G., & Broich, M. (2017). Modeling multidecadal surface water inundation dynamics and key drivers on large river basin scale using multiple time series of Earth-observation and river flow data. *Water Resources Research*, 53, 1251–1269. <https://doi.org/10.1002/2016WR019858>

- Hirpa, F. A., Hopson, T. M., De Groot, T., Brakenridge, G. R., Gebremichael, M., & Restrepo, P. J. (2013). Upstream satellite remote sensing for river discharge forecasting: Application to major rivers in South Asia. *Remote Sensing of Environment*, 131, 140–151. <https://doi.org/10.1016/j.rse.2012.11.013>
- Huang, C., Chen, Y., & Wu, J. (2013). *GIS-based spatial zoning for flood inundation modelling in the Murray-Darling Basin*. Paper presented at 20th International Congress on Modelling and Simulation, Adelaide, Australia.
- Huang, C., Chen, Y., & Wu, J. (2014a). Mapping spatio-temporal flood inundation dynamics at large river basin scale using time-series flow data and MODIS imagery. *International Journal of Applied Earth Observation and Geoinformation*, 26(0), 350–362. <https://doi.org/10.1016/j.jag.2013.09.002>
- Huang, C., Chen, Y., & Wu, J. (2014b). DEM-based modification of pixel-swapping algorithm for enhancing floodplain inundation mapping. *International Journal of Remote Sensing*, 35(1), 365–381. <https://doi.org/10.1080/01431161.2013.871084>
- Huang, C., Chen, Y., Wu, J., Chen, Z., Li, L., Liu, R., & Yu, J. (2014). *Integration of remotely sensed inundation extent and high-precision topographic data for mapping inundation depth*. Paper presented at The Third International Conference on Agro-Geoinformatics, Beijing, China.
- Huang, C., Chen, Y., Wu, J., Li, L., & Liu, R. (2015). An evaluation of Suomi NPP-VIIRS data for surface water detection. *Remote Sensing Letters*, 6(2), 155–164. <https://doi.org/10.1080/2150704X.2015.1017664>
- Huang, C., Chen, Y., Zhang, S., Li, L., Shi, K., & Liu, R. (2016). Surface water mapping from Suomi NPP-VIIRS imagery at 30 m resolution via blending with Landsat data. *Remote Sensing*, 8(8), 631.
- Huang, C., Chen, Y., Zhang, S., Li, L., Shi, K., & Liu, R. (2017). Spatial downscaling of Suomi NPP-VIIRS image for lake mapping. *Water*, 9(11), 834. <https://doi.org/10.3390/w9110834>
- Huang, C., Nguyen, B. D., Zhang, S., Cao, S., & Wagner, W. (2017). A comparison of terrain indices toward their ability in assisting surface water mapping from Sentinel-1 data. *ISPRS International Journal of Geographical Information*, 6(5), 140.
- Huang, C., Peng, Y., Lang, M., Yeo, I.-Y., & McCarty, G. (2014). Wetland inundation mapping and change monitoring using Landsat and airborne LiDAR data. *Remote Sensing of Environment*, 141, 231–242. <https://doi.org/10.1016/j.rse.2013.10.020>
- Huang, C., Zan, X., Yang, X., & Zhang, S. (2016). *Surface water change detection using change vector analysis*. Paper presented at IEEE International Geoscience and Remote Sensing Symposium (IGARSS2016), Beijing, China.
- Hui, F. M., Xu, B., Huang, H. B., Yu, Q., & Gong, P. (2008). Modelling spatial-temporal change of Poyang Lake using multitemporal Landsat imagery. *International Journal of Remote Sensing*, 29(20), 5767–5784. <https://doi.org/10.1080/01431160802060912>
- Ichoku, C., & Karniel, A. (1996). A review of mixture modeling techniques for sub-pixel land cover estimation. *Remote Sensing Reviews*, 13(3-4), 161–186. <https://doi.org/10.1080/02757259609532303>
- Isikdogan, F., Bovik, A., & Passalacqua, P. (2017). RivaMap: An automated river analysis and mapping engine. *Remote Sensing of Environment*, 202(Supplement C), 88–97. <https://doi.org/10.1016/j.rse.2017.03.044>
- Islam, A. S., Bala, S. K., & Haque, M. A. (2010). Flood inundation map of Bangladesh using MODIS time-series images. *Journal of Flood Risk Management*, 3(3), 210–222. <https://doi.org/10.1111/j.1753-318X.2010.01074.x>
- Islam, M. D. M., & Sado, K. (2000). Development of flood hazard maps of Bangladesh using NOAA-AVHRR images with GIS. *Hydrological Sciences Journal*, 45(3), 337–355. <https://doi.org/10.1080/0262660009492334>
- Jain, S. K., Saraf, A. K., Goswami, A., & Ahmad, T. (2006). Flood inundation mapping using NOAA AVHRR data. *Water Resources Management*, 20(6), 949–959. <https://doi.org/10.1007/s11269-006-9016-4>
- Jarihani, A. A., McVicar, T. R., Van Niel, T. G., Emelyanova, I. V., Callow, J. N., & Johansen, K. (2014). Blending Landsat and MODIS data to generate multispectral indices: a comparison of “index-then-blend” and “blend-then-index” approaches. *Remote Sensing*, 6(10), 9213–9238. <https://doi.org/10.3390/rs6109213>
- Ji, L., Zhang, L., & Wylie, B. (2009). Analysis of dynamic thresholds for the normalized difference water index. *Photogrammetric Engineering and Remote Sensing*, 75(11), 1307–1317.
- Ji, L. Y., Geng, X. R., Sun, K., Zhao, Y. C., & Gong, P. (2015). Target detection method for water mapping using Landsat 8 OLI/TIRS imagery. *Water*, 7(2), 794–817. <https://doi.org/10.3390/w7020794>
- Jiang, H., Feng, M., Zhu, Y., Lu, N., Huang, J., & Xiao, T. (2014). An automated method for extracting rivers and lakes from Landsat imagery. *Remote Sensing*, 6(6), 5067–5089.
- Jin, H., Huang, C., Lang, M. W., Yeo, I.-Y., & Stehman, S. V. (2017). Monitoring of wetland inundation dynamics in the Delmarva Peninsula using Landsat time-series imagery from 1985 to 2011. *Remote Sensing of Environment*, 190(Supplement C), 26–41. <https://doi.org/10.1016/j.rse.2016.12.001>
- Joshi, N., Baumann, M., Ehammer, A., Fenstolt, R., Grogan, K., Hostert, P., et al. (2016). A review of the application of optical and radar remote sensing data fusion to land use mapping and monitoring. *Remote Sensing*, 8(1), 70.
- Karpantne, A., Khandelwal, A., Chen, X., Mithal, V., Faghmous, J., & Kumar, V. (2016). Global monitoring of inland water dynamics: State-of-the-art, challenges, and opportunities. In J. Lässig, K. Kersting, & K. Morik (Eds.), *Computational Sustainability* (pp. 121–147). Cham: Springer International Publishing.
- Khandelwal, A., Karpantne, A., Marlier, M. E., Kim, J., Lettenmaier, D. P., & Kumar, V. (2017). An approach for global monitoring of surface water extent variations in reservoirs using MODIS data. *Remote Sensing of Environment*, 202(Supplement C), 113–128. <https://doi.org/10.1016/j.rse.2017.05.039>
- Klemenjak, S., Waske, B., Valero, S., & Chanussot, J. (2012). *Unsupervised river detection in RapidEye data*. Paper presented at IEEE International Geoscience and Remote Sensing Symposium (IGARSS2012), Munich, Germany.
- Ko, B., Kim, H., & Nam, J. (2015). Classification of potential water bodies using Landsat 8 OLI and a combination of two boosted Random Forest classifiers. *Sensors*, 15(6), 13763.
- Landmann, T., Schramm, M., Huettich, C., & Dech, S. (2013). MODIS-based change vector analysis for assessing wetland dynamics in Southern Africa. *Remote Sensing Letters*, 4(2), 104–113.
- Lang, M., & McCarty, G. (2009). Lidar intensity for improved detection of inundation below the forest canopy. *Wetlands*, 29(4), 1166–1178. <https://doi.org/10.1672/08-197.1>
- Leauthaud, C., Belaud, G., Duvail, S., Moussa, R., Grunberger, O., & Albergel, J. (2013). Characterizing floods in the poorly gauged wetlands of the Tana river delta, Kenya, using a water balance model and satellite data. *Hydrology and Earth System Sciences*, 17(8), 3059–3075. <https://doi.org/10.5194/hess-17-3059-2013>
- Lee, H., Durand, M., Jung, H. C., Alsdorf, D., Shum, C. K., & Sheng, Y. (2010). Characterization of surface water storage changes in Arctic lakes using simulated SWOT measurements. *International Journal of Remote Sensing*, 31(14), 3931–3953. <https://doi.org/10.1080/01431161.2010.483494>
- LeFavour, G., & Alsdorf, D. (2005). Water slope and discharge in the Amazon River estimated using the shuttle radar topography mission digital elevation model. *Geophysical Research Letters*, 32, L17404. <https://doi.org/10.1029/2005GL023836>

- Legleiter, C. J. (2015). Calibrating remotely sensed river bathymetry in the absence of field measurements: Flow REsistance Equation-Based Imaging of River Depths (FREEBIRD). *Water Resources Research*, 51, 2865–2884. <https://doi.org/10.1002/2014WR016624>
- Legleiter, C. J., Roberts, D. A., & Lawrence, R. L. (2009). Spectrally based remote sensing of river bathymetry. *Earth Surface Processes and Landforms*, 34(8), 1039–1059. <https://doi.org/10.1002/esp.1787>
- Lewis, A., Oliver, S., Lymburner, L., Evans, B., Wyborn, L., Mueller, N., et al. (2017). The Australian Geoscience Data Cube—Foundations and lessons learned. *Remote Sensing of Environment*, 202, 276–292. <https://doi.org/10.1016/j.rse.2017.03.015>
- Li, J. L., & Sheng, Y. W. (2012). An automated scheme for glacial lake dynamics mapping using Landsat imagery and digital elevation models: A case study in the Himalayas. *International Journal of Remote Sensing*, 33(16), 5194–5213. <https://doi.org/10.1080/01431161.2012.657370>
- Li, L., Chen, Y., Yu, X., Liu, R., & Huang, C. (2015). Sub-pixel flood inundation mapping from multispectral remotely sensed images based on discrete particle swarm optimization. *ISPRS Journal of Photogrammetry and Remote Sensing*, 101(0), 10–21. <https://doi.org/10.1016/j.isprsjprs.2014.11.006>
- Li, S., Sun, D., Goldberg, M., & Stefanidis, A. (2013). Derivation of 30-m-resolution water maps from TERRA/MODIS and SRTM. *Remote Sensing of Environment*, 134, 417–430. <https://doi.org/10.1016/j.rse.2013.03.015>
- Li, S., Sun, D., Goldberg, M. D., Sjoberg, B., Santek, D., Hoffman, J. P., et al. (2018). Automatic near real-time flood detection using Suomi-NPP/VIIRS data. *Remote Sensing of Environment*, 204(Supplement C), 672–689. <https://doi.org/10.1016/j.rse.2017.09.032>
- Li, S., Sun, D., & Yu, Y. (2013). Automatic cloud-shadow removal from flood/standing water maps using MSG/SEVIRI imagery. *International Journal of Remote Sensing*, 34(15), 5487–5502. <https://doi.org/10.1080/01431161.2013.792969>
- Li, S., Sun, D., Yu, Y., Csizsar, I., Stefanidis, A., & Goldberg, M. D. (2013). A new Short-Wave Infrared (SWIR) method for quantitative water fraction derivation and evaluation with EOS/MODIS and Landsat/TM data. *IEEE Transactions on Geoscience and Remote Sensing*, 51(3), 1852–1862. <https://doi.org/10.1109/tgrs.2012.2208466>
- Li, Y., Gong, X., Guo, Z., Xu, K., Hu, D., & Zhou, H. (2016). An index and approach for water extraction using Landsat-OLI data. *International Journal of Remote Sensing*, 37(16), 3611–3635. <https://doi.org/10.1080/01431161.2016.1201228>
- Liao, A. P., Chen, L. J., Chen, J., He, C. Y., Xin, C., Jin, C., et al. (2014). High-resolution remote sensing mapping of global land water. *Science China Earth Sciences*, 57(10), 2305–2316.
- Ling, F., Du, Y., Xiao, F., Xue, H. P., & Wu, S. J. (2010). Super-resolution land-cover mapping using multiple sub-pixel shifted remotely sensed images. *International Journal of Remote Sensing*, 31(19), 5023–5040. <https://doi.org/10.1080/01431160903252350>
- Ling, F., Li, W., Du, Y., & Li, X. (2011). Land cover change mapping at the subpixel scale with different spatial-resolution remotely sensed imagery. *IEEE Geoscience and Remote Sensing*, 8(1), 182–186. <https://doi.org/10.1109/LGRS.2010.2055034>
- Ling, F., Li, X. D., Du, Y., & Xiao, F. (2013). Sub-pixel mapping of remotely sensed imagery with hybrid intra- and inter-pixel dependence. *International Journal of Remote Sensing*, 34(1), 341–357. <https://doi.org/10.1080/01431161.2012.705441>
- Ling, F., Xiao, F., Du, Y., Xue, H. P., & Ren, X. Y. (2008). Waterline mapping at the subpixel scale from remote sensing imagery with high-resolution digital elevation models. *International Journal of Remote Sensing*, 29(6), 1809–1815. <https://doi.org/10.1080/01431160701802489>
- Liu, Z., Yao, Z., & Wang, R. (2016). Assessing methods of identifying open water bodies using Landsat 8 OLI imagery. *Environment and Earth Science*, 75(10), 1–13.
- López-Caloca, A., Tapia-Silva, F.-O., & Escalante-Ramírez, B. (2008). *Lake Chapala change detection using time series*. Paper presented at SPIE Remote Sensing, Cardiff, United Kingdom
- Lu, S., Jia, L., Zhang, L., Wei, Y., Baig, M. H. A., Zhai, Z., et al. (2017). Lake water surface mapping in the Tibetan Plateau using the MODIS MOD09Q1 product. *Remote Sensing Letters*, 8(3), 224–233. <https://doi.org/10.1080/2150704X.2016.1260178>
- Lu, S., Wu, B., Yan, N., & Wang, H. (2011). Water body mapping method with HJ-1A/B satellite imagery. *International Journal of Applied Earth Observation and Geoinformation*, 13(3), 428–434. <https://doi.org/10.1016/j.jag.2010.09.006>
- Malinowski, R., Groom, G., Schwanghart, W., & Heckrath, G. (2015). Detection and delineation of localized flooding from WorldView-2 multi-spectral Remote Sensing, 7(11), 14853.
- Manavalan, P., Sathyathan, P., & Rajegowda, G. L. (1993). Digital image analysis techniques to estimate waterspread for capacity evaluations of reservoirs. *Photogrammetric Engineering and Remote Sensing*, 59(9), 1389–1395.
- McFeeters, S. K. (1996). The use of the normalized difference water index (NDWI) in the delineation of open water features. *International Journal of Remote Sensing*, 17(7), 1425–1432.
- McGinnis, D. F., & Rango, A. (1975). Earth Resources Satellite Systems for flood monitoring. *Geophysical Research Letters*, 2(4), 132–135. <https://doi.org/10.1029/GL002i004p00132>
- Mercury, M., Green, R., Hook, S., Oaida, B., Wu, W., Gunderson, A., & Chodas, M. (2012). Global cloud cover for assessment of optical satellite observation opportunities: A HyspIRI case study. *Remote Sensing of Environment*, 126(Supplement C), 62–71. <https://doi.org/10.1016/j.rse.2012.08.007>
- Mertens, K. C., De Baets, B., Verbeke, L. P. C., & De Wulf, R. R. (2006). A sub-pixel mapping algorithm based on sub-pixel/pixel spatial attraction models. *International Journal of Remote Sensing*, 27(15), 3293–3310. <https://doi.org/10.1080/01431160500497127>
- Mertens, K. C., Verbeke, L. P. C., Ducheyne, E. I., & De Wulf, R. R. (2003). Using genetic algorithms in sub-pixel mapping. *International Journal of Remote Sensing*, 24(21), 4241–4247. <https://doi.org/10.1080/01431160310001595073>
- Mohammadi, A., Costelloe, J. F., & Ryu, D. (2017). Application of time series of remotely sensed normalized difference water, vegetation and moisture indices in characterizing flood dynamics of large-scale arid zone floodplains. *Remote Sensing of Environment*, 190, 70–82. <https://doi.org/10.1016/j.rse.2016.12.003>
- Mueller, N., Lewis, A., Roberts, D., Ring, S., Melrose, R., Sixsmith, J., et al. (2016). Water observations from space: Mapping surface water from 25 years of Landsat imagery across Australia. *Remote Sensing of Environment*, 174, 341–352. <https://doi.org/10.1016/j.rse.2015.11.003>
- Nash, J. E., & Sutcliffe, J. V. (1970). River flow forecasting through conceptual models part I - A discussion of principles. *Journal of Hydrology*, 10(3), 282–290. [https://doi.org/10.1016/0022-1694\(70\)90255-6](https://doi.org/10.1016/0022-1694(70)90255-6)
- Nyborg, L., & Sandholt, I. (2001). *NOAA-AVHRR based flood monitoring*. Paper presented at IEEE International Geoscience and Remote Sensing Symposium (IGARSS2001), Sydney, Australia.
- Ogilvie, A., Belaud, G., Delenne, C., Bailly, J.-S., Bader, J.-C., Oleksiak, A., et al. (2015). Decadal monitoring of the Niger Inner Delta flood dynamics using MODIS optical data. *Journal of Hydrology*, 523, 368–383. <https://doi.org/10.1016/j.jhydrol.2015.01.036>
- Olthof, I. (2017). Mapping seasonal inundation frequency (1985–2016) along the St-John River, New Brunswick, Canada using the Landsat archive. *Remote Sensing*, 9(2), 143.
- Ordoyne, C., & Friedl, M. A. (2008). Using MODIS data to characterize seasonal inundation patterns in the Florida Everglades. *Remote Sensing of Environment*, 112(11), 4107–4119. <https://doi.org/10.1016/j.rse.2007.08.027>

- Ouma, Y. O., & Tateishi, R. (2006). A water index for rapid mapping of shoreline changes of five East African Rift Valley lakes: An empirical analysis using Landsat TM and ETM+ data. *International Journal of Remote Sensing*, 27(15), 3153–3181. <https://doi.org/10.1080/01431160500309934>
- Overton, I. C. (2005). Modelling floodplain inundation on a regulated river: Integrating GIS, remote sensing and hydrological models. *River Research and Applications*, 21(9), 991–1001. <https://doi.org/10.1002/rra.867>
- Ozesmi, S. L., & Bauer, M. E. (2002). Satellite remote sensing of wetlands. *Wetlands Ecology and Management*, 10(5), 381–402. <https://doi.org/10.1023/a:1020908432489>
- Papa, F., Frappart, F., Guntner, A., Prigent, C., Aires, F., Getirana, A., & Maurer, R. (2013). Surface freshwater storage and variability in the Amazon basin from multi-satellite observations, 1993–2007. *Journal of Geophysical Research: Atmospheres*, 118, 11,951–11,965. <https://doi.org/10.1029/2013JD020500>
- Papa, F., Prigent, C., Aires, F., Jimenez, C., Rossow, W., & Matthews, E. (2010). Interannual variability of surface water extent at the global scale, 1993–2004. *Journal of Geophysical Research*, 115, D12111. <https://doi.org/10.1029/2009JD012674>
- Papa, F., Prigent, C., & Rossow, W. B. (2008). Monitoring flood and discharge variations in the large Siberian rivers from a multi-satellite technique. *Surveys in Geophysics*, 29(4–5), 297–317. <https://doi.org/10.1007/s10712-008-9036-0>
- Pardo-Pascual, J. E., Almonacid-Caballer, J., Ruiz, L. A., & Palomar-Vazquez, J. (2012). Automatic extraction of shorelines from Landsat TM and ETM+ multi-temporal images with subpixel precision. *Remote Sensing of Environment*, 123, 1–11. <https://doi.org/10.1016/j.rse.2012.02.024>
- Pavelsky, T. M. (2014). Using width-based rating curves from spatially discontinuous satellite imagery to monitor river discharge. *Hydrological Processes*, 28(6), 3035–3040. <https://doi.org/10.1002/hyp.10157>
- Pavelsky, T. M., Durand, M. T., Andreidis, K. M., Beighley, R. E., Paiva, R. C. D., Allen, G. H., & Miller, Z. F. (2014). Assessing the potential global extent of SWOT river discharge observations. *Journal of Hydrology*, 519(Part B), 1516–1525. <https://doi.org/10.1016/j.jhydrol.2014.08.044>
- Pavelsky, T. M., & Smith, L. C. (2008a). RivWidth: A software tool for the calculation of river widths from remotely sensed imagery. *IEEE Geoscience and Remote Sensing*, 5(1), 70–73. <https://doi.org/10.1109/LGRS.2007.908305>
- Pavelsky, T. M., & Smith, L. C. (2008b). Remote sensing of hydrologic recharge in the Peace-Athabasca Delta, Canada. *Geophysical Research Letters*, 35, L08403. <https://doi.org/10.1029/2008GL033268>
- Pekel, J.-F., Cottam, A., Gorelick, N., & Belward, A. S. (2016). High-resolution mapping of global surface water and its long-term changes. *Nature*, 540(7633), 418.
- Peng, D. Z., Xiong, L. H., Guo, S. L., & Shu, N. (2005). Study of Dongting Lake area variation and its influence on water level using MODIS data. *Hydrological Sciences Journal*, 50(1), 31–44. <https://doi.org/10.1623/hysj.50.1.31.56327>
- Penton, D. J., & Overton, I. C. (2007). Spatial modelling of floodplain inundation combining satellite imagery and elevation models. Paper presented at International Congress on Modelling and Simulation (MODSIM2007), Christchurch, New Zealand.
- Plumb, E. (2015). River ice and flood detection products derived from Suomi NPP VIIRS satellite data to support hydrologic forecast operations in Alaska. Paper presented at 2015 AGU Fall Meeting, San Francisco, USA.
- Prigent, C., Lettenmaier, D. P., Aires, F., & Papa, F. (2016). Toward a high-resolution monitoring of continental surface water extent and dynamics at global scale: from GIEMS (Global Inundation Extent from Multi-Satellites) to SWOT (Surface Water Ocean Topography). *Surveys in Geophysics*, 37(2), 339–355. <https://doi.org/10.1007/s10712-015-9339-x>
- Prigent, C., Matthews, E., Aires, F., & Rossow, W. B. (2001). Remote sensing of global wetland dynamics with multiple satellite data sets. *Geophysical Research Letters*, 28(24), 4631–4634. <https://doi.org/10.1029/2001GL013263>
- Prigent, C., Papa, F., Aires, F., Rossow, W. B., & Matthews, E. (2007). Global inundation dynamics inferred from multiple satellite observations, 1993–2000. *Journal of Geophysical Research*, 112, D12107. <https://doi.org/10.1029/2006JD007847>
- Qi, S. H., Brown, D. G., Tian, Q., Jiang, L. G., Zhao, T. T., & Bergen, K. A. (2009). Inundation extent and flood frequency mapping using LANDSAT imagery and Digital Elevation Models. *GIScience & Remote Sensing*, 46(1), 101–127. <https://doi.org/10.2747/1548-1603.46.1.101>
- Rennó, C. D., Nobre, A. D., Cuartas, L. A., Soares, J. V., Hodnett, M. G., Tomasella, J., & Waterloo, M. J. (2008). HAND, a new terrain descriptor using SRTM-DEM: Mapping terra-firme rainforest environments in Amazonia. *Remote Sensing of Environment*, 112(9), 3469–3481. <https://doi.org/10.1016/j.rse.2008.03.018>
- Ringeval, B., De Nobletducouadre, N., Ciais, P., Bousquet, P., Prigent, C., Papa, F., & Rossow, W. B. (2010). An attempt to quantify the impact of changes in wetland extent on methane emissions on the seasonal and interannual time scales. *Global Biogeochemical Cycles*, 24, GB2003. <https://doi.org/10.1029/2008GB003354>
- Rokni, K., Ahmad, A., Selamat, A., & Hazini, S. (2014). Water feature extraction and change detection using multitemporal Landsat imagery. *Remote Sensing*, 6(5), 4173–4189.
- Sagin, J., Sizo, A., Wheeler, H., Jardine, T. D., & Lindenschmidt, K. E. (2015). A water coverage extraction approach to track inundation in the Saskatchewan River Delta, Canada. *International Journal of Remote Sensing*, 36(3), 764–781. <https://doi.org/10.1080/01431161.2014.1001084>
- Sakamoto, T., Van Nguyen, N., Kotera, A., Ohno, H., Ishitsuka, N., & Yokozawa, M. (2007). Detecting temporal changes in the extent of annual flooding within the Cambodia and the Vietnamese Mekong Delta from MODIS time-series imagery. *Remote Sensing of Environment*, 109(3), 295–313. <https://doi.org/10.1016/j.rse.2007.01.011>
- Salomonson, V. V., & Appel, I. (2004). Estimating fractional snow cover from MODIS using the normalized difference snow index. *Remote Sensing of Environment*, 89(3), 351–360. <https://doi.org/10.1016/j.rse.2003.10.016>
- Sawaya, K. E., Olmanson, L. G., Heinert, N. J., Brezonik, P. L., & Bauer, M. E. (2003). Extending satellite remote sensing to local scales: Land and water resource monitoring using high-resolution imagery. *Remote Sensing of Environment*, 88(1–2), 144–156. <https://doi.org/10.1016/j.rse.2003.04.006>
- Schaffer-Smith, D., Swenson, J. J., Barbaree, B., & Reiter, M. E. (2017). Three decades of Landsat-derived spring surface water dynamics in an agricultural wetland mosaic: Implications for migratory shorebirds. *Remote Sensing of Environment*, 193, 180–192. <https://doi.org/10.1016/j.rse.2017.02.016>
- Schumann, G., Bates, P. D., Horritt, M. S., Matgen, P., & Pappenberger, F. (2009). Progress in integration of remote sensing-derived flood extent and stage data and hydraulic models. *Reviews of Geophysics*, 47, RG4001. <https://doi.org/10.1029/2008RG000274>
- Schumann, G. J. P., & Moller, D. K. (2015). Microwave remote sensing of flood inundation. *Physics and Chemistry of the Earth*, 83–84, 84–95. <https://doi.org/10.1016/j.pce.2015.05.002>
- Shah, C. A. (2011). Automated lake shoreline mapping at subpixel accuracy. *IEEE Geoscience and Remote Sensing*, 8(6), 1125–1129. <https://doi.org/10.1109/LGRS.2011.2157951>
- Sharma, R., Tateishi, R., Hara, K., & Nguyen, L. (2015). Developing Superfine Water Index (SWI) for global water cover mapping using MODIS data. *Remote Sensing*, 7(10), 13807.

- Sheng, Y., Gong, P., & Xiao, Q. (2001). Quantitative dynamic flood monitoring with NOAA AVHRR. *International Journal of Remote Sensing*, 22(9), 1709–1724. <https://doi.org/10.1080/01431160118481>
- Sheng, Y., Shah, C. A., & Smith, L. C. (2008). Automated image registration for hydrologic change detection in the lake-rich Arctic. *IEEE Geoscience and Remote Sensing*, 5(3), 414–418.
- Sheng, Y., Song, C., Wang, J., Lyons, E. A., Knox, B. R., Cox, J. S., & Gao, F. (2016). Representative lake water extent mapping at continental scales using multi-temporal Landsat-8 imagery. *Remote Sensing of Environment*, 185, 129–141. <https://doi.org/10.1016/j.rse.2015.12.041>
- Sheng, Y. W., Su, Y. F., & Xiao, Q. G. (1998). Challenging the cloud-contamination problem in flood monitoring with NOAA/AVHRR imagery. *Photogrammetric Engineering and Remote Sensing*, 64(3), 191–198.
- Sichangi, A. W., Wang, L., Yang, K., Chen, D., Wang, Z., Li, X., et al. (2016). Estimating continental river basin discharges using multiple remote sensing data sets. *Remote Sensing of Environment*, 179(Supplement C), 36–53. <https://doi.org/10.1016/j.rse.2016.03.019>
- Sidle, R. C., Ziegler, A. D., & Vogler, J. B. (2007). Contemporary changes in open water surface area of Lake Inle, Myanmar. *Sustainability Science*, 2(1), 55–65. <https://doi.org/10.1007/s11625-006-0020-7>
- Sims, N., Warren, G., Overton, I., Austin, J., Gallant, J., King, D., et al. (2014). *RiM-FIM floodplain inundation modelling for the Edward-Wakool, Lower Murrumbidgee and Lower Darling River systems, Water for a Healthy Country Flagship Report series*. Clayton, Australia: CSIRO.
- Singh, K., Ghosh, M., & Sharma, S. R. (2016). WSB-DA: Water Surface Boundary Detection Algorithm using Landsat 8 OLI data. *IEEE Journal of Selected Topics Applied Earth Observation Remote Sensing*, 9(1), 363–368. <https://doi.org/10.1109/JSTARS.2015.2504338>
- Sivanpillai, R., & Miller, S. N. (2010). Improvements in mapping water bodies using ASTER data. *Ecological Informatics*, 5(1), 73–78. <https://doi.org/10.1016/j.ecoinf.2009.09.013>
- Smith, L. C. (1997). Satellite remote sensing of river inundation area, stage, and discharge: A review. *Hydrological Processes*, 11(10), 1427–1439.
- Smith, L. C., Isacks, B. L., Bloom, A. L., & Murray, A. B. (1996). Estimation of discharge from three braided rivers using synthetic aperture radar satellite imagery: Potential application to ungaged basins. *Water Resources Research*, 32(7), 2021–2034. <https://doi.org/10.1029/96WR00752>
- Smith, L. C., Isacks, B. L., Forster, R. R., Bloom, A. L., & Preuss, I. (1995). Estimation of discharge from braided glacial rivers using ERS-1 Synthetic-Aperture Radar—First results. *Water Resources Research*, 31(5), 1325–1329. <https://doi.org/10.1029/95WR00145>
- Smith, L. C., & Pavelsky, T. M. (2008). Estimation of river discharge, propagation speed, and hydraulic geometry from space: Lena River, Siberia. *Water Resources Research*, 44, W03427. <https://doi.org/10.1029/2007WR006133>
- Soti, V., Tran, A., Baily, J. S., Puech, C., Lo Seen, D., & Begue, A. (2009). Assessing optical Earth observation systems for mapping and monitoring temporary ponds in arid areas. *International Journal of Applied Earth Observation and Geoinformation*, 11(5), 344–351. <https://doi.org/10.1016/j.jag.2009.05.005>
- Sun, D. L., Yu, Y. Y., & Goldberg, M. D. (2011). Deriving water fraction and flood maps from MODIS images using a decision tree approach. *IEEE Journal of Selected Topics Applied Earth Observation Remote Sensing*, 4(4), 814–825. <https://doi.org/10.1109/JSTARS.2011.2125778>
- Tarpanelli, A., Amarnath, G., Brocca, L., Massari, C., & Moramarco, T. (2017). Discharge estimation and forecasting by MODIS and altimetry data in Niger-Benue River. *Remote Sensing of Environment*, 195, 96–106. <https://doi.org/10.1016/j.rse.2017.04.015>
- Tarpanelli, A., Brocca, L., Lacava, T., Faruolo, M., Melone, F., Moramarco, T., et al. (2011). River discharge estimation through MODIS data. In C. M. U. Neale & A. Maltese (Eds.), *SPIE Remote Sensing for Agriculture, Ecosystems, and Hydrology XIII* (pp. 283–304). Czech Republic: Prague.
- Tarpanelli, A., Brocca, L., Lacava, T., Melone, F., Moramarco, T., Faruolo, M., et al. (2013). Toward the estimation of river discharge variations using MODIS data in ungauged basins. *Remote Sensing of Environment*, 136(0), 47–55. <https://doi.org/10.1016/j.rse.2013.04.010>
- Tatem, A. J., Lewis, H. G., Atkinson, P. M., & Nixon, M. S. (2002). Super-resolution land cover pattern prediction using a Hopfield neural network. *Remote Sensing of Environment*, 79(1), 1–14. [https://doi.org/10.1016/s0034-4257\(01\)00229-2](https://doi.org/10.1016/s0034-4257(01)00229-2)
- Thito, K., Wolksi, P., & Murray-Hudson, M. (2016). Mapping inundation extent, frequency and duration in the Okavango Delta from 2001 to 2012. *African Journal of Aquatic Science*, 41(3), 267–277. <https://doi.org/10.2989/16085914.2016.1173009>
- Thomas, R. F., Kingsford, R. T., Lu, Y., & Hunter, S. J. (2011). Landsat mapping of annual inundation (1979–2006) of the Macquarie Marshes in semi-arid Australia. *International Journal of Remote Sensing*, 32(16), 4545–4569. <https://doi.org/10.1080/01431161.2010.489064>
- Townsend, P. A., & Walsh, S. J. (1998). Modeling floodplain inundation using an integrated GIS with radar and optical remote sensing. *Geomorphology*, 21(3–4), 295–312. [https://doi.org/10.1016/s0169-555x\(97\)00069-x](https://doi.org/10.1016/s0169-555x(97)00069-x)
- Tulbure, M. G., & Broich, M. (2013). Spatiotemporal dynamic of surface water bodies using Landsat time-series data from 1999 to 2011. *ISPRS Journal of Photogrammetry and Remote Sensing*, 79, 44–52. <https://doi.org/10.1016/j.isprsjprs.2013.01.010>
- Tulbure, M. G., Broich, M., Stehman, S. V., & Kammareddy, A. (2016). Surface water extent dynamics from three decades of seasonally continuous Landsat time series at subcontinental scale in a semi-arid region. *Remote Sensing of Environment*, 178, 142–157. <https://doi.org/10.1016/j.rse.2016.02.034>
- Verpoorter, C., Kutser, T., Seekell, D. A., & Tranvik, L. J. (2014). A global inventory of lakes based on high-resolution satellite imagery. *Geophysical Research Letters*, 41, 6396–6402. <https://doi.org/10.1002/2014GL060641>
- Vörösmarty, C. J., Green, P., Salisbury, J., & Lammers, R. B. (2000). Global water resources: Vulnerability from climate change and population growth. *Science*, 289(5477), 284–288. <https://doi.org/10.1126/science.289.5477.284>
- Vörösmarty, C. J., McIntyre, P. B., Gessner, M. O., Dudgeon, D., Prusevich, A., Green, P., et al. (2010). Global threats to human water security and river biodiversity. *Nature*, 467(7315), 555–561.
- Wang, Y. (2002). Mapping extent of floods: What we have learned and how we can do better. *Natural Hazards Review*, 3(2), 68–73. [https://doi.org/10.1061/\(ASCE\)1527-6988\(2002\)3:2\(68\)](https://doi.org/10.1061/(ASCE)1527-6988(2002)3:2(68))
- Wang, Y. (2004). Using Landsat 7 TM data acquired days after a flood event to delineate the maximum flood extent on a coastal floodplain. *International Journal of Remote Sensing*, 25(5), 959–974.
- Wang, S., Baig, M. H. A., Zhang, L., Jiang, H., Ji, Y., Zhao, H., & Tian, J. (2015). A simple enhanced water index (EWI) for percent surface water estimation using Landsat data. *IEEE Journal of Selected Topics Applied Earth Observation Remote Sensing*, 8(1), 90–97. <https://doi.org/10.1109/JSTARS.2014.2387196>
- Wang, Y., Colby, J. D., & Mulcahy, K. A. (2002). An efficient method for mapping flood extent in a coastal floodplain using Landsat TM and DEM data. *International Journal of Remote Sensing*, 23(18), 3681–3696. <https://doi.org/10.1080/01431160110114484>
- Wania, R., Melton, J. R., Hodson, E. L., Poultier, B., Ringeval, B., Spahni, R., et al. (2012). Present state of global wetland extent and wetland methane modelling: Methodology of a model inter-comparison project (WETCHIMP). *Geoscientific Model Development*, 6(3), 617–641.
- Ward, D. P., Petty, A., Setterfield, S. A., Douglas, M. M., Ferdinand, K., Hamilton, S. K., & Phinn, S. (2014). Floodplain inundation and vegetation dynamics in the Alligator Rivers region (Kakadu) of northern Australia assessed using optical and radar remote sensing. *Remote Sensing of Environment*, 147(Supplement C), 43–55. <https://doi.org/10.1016/j.rse.2014.02.009>

- Whitcomb, J., Moghaddam, M., McDonald, K., Kellndorfer, J., & Podest, E. (2009). Mapping vegetated wetlands of Alaska using L-band radar satellite imagery. *Canadian Journal of Remote Sensing*, 35(1), 54–72. <https://doi.org/10.5589/m08-080>
- Wu, G., & Liu, Y. (2016). Mapping dynamics of inundation patterns of two largest river-connected lakes in China: A comparative study. *Remote Sensing*, 8(7), 560.
- Wu, P., Shen, H., Zhang, L., & Götsche, F. M. (2015). Integrated fusion of multi-scale polar-orbiting and geostationary satellite observations for the mapping of high spatial and temporal resolution land surface temperature. *Remote Sensing of Environment*, 156, 169–181.
- Wylie, D., Jackson, D. L., Menzel, W. P., & Bates, J. J. (2005). Trends in global cloud cover in two decades of HIRS observations. *Journal of Climate*, 18(15), 3021–3031. <https://doi.org/10.1175/JCLI3461.1>
- Xiao, X., Boles, S., Froliking, S., Salas, W., Moore, B., Li, C., et al. (2002). Observation of flooding and rice transplanting of paddy rice fields at the site to landscape scales in China using VEGETATION sensor data. *International Journal of Remote Sensing*, 23(15), 3009–3022. <https://doi.org/10.1080/01431160110107734>
- Xie, C., Huang, X., Zeng, W., & Fang, X. (2016). A novel water index for urban high-resolution eight-band WorldView-2 imagery. *International Journal of Digital Earth*, 9(10), 925–941. <https://doi.org/10.1080/17538947.2016.1170215>
- Xie, H., Luo, X., Xu, X., Pan, H., & Tong, X. (2016). Evaluation of Landsat 8 OLI imagery for unsupervised inland water extraction. *International Journal of Remote Sensing*, 37(8), 1826–1844. <https://doi.org/10.1080/01431161.2016.1168948>
- Xu, H. Q. (2006). Modification of normalised difference water index (NDWI) to enhance open water features in remotely sensed imagery. *International Journal of Remote Sensing*, 27(14), 3025–3033.
- Xu, K., Zhang, J., Watanabe, M., & Sun, C. (2004). Estimating river discharge from very high-resolution satellite data: a case study in the Yangtze River, China. *Hydrological Processes*, 18(10), 1927–1939. <https://doi.org/10.1002/hyp.1458>
- Yamazaki, D., Ikeshima, D., Tawatari, R., Yamaguchi, T., O'Loughlin, F., Neal, J. C., et al. (2017). A high-accuracy map of global terrain elevations. *Geophysical Research Letters*, 44, 5844–5853. <https://doi.org/10.1002/2017GL072874>
- Yamazaki, D., & Trigg, M. A. (2016). Hydrology: The dynamics of Earth's surface water. *Nature*, 540(7633), 348–349.
- Yan, Y. E., Ouyang, Z. T., Guo, H. Q., Jin, S. S., & Zhao, B. (2010). Detecting the spatiotemporal changes of tidal flood in the estuarine wetland by using MODIS time series data. *Journal of Hydrology*, 384(1–2), 156–163. <https://doi.org/10.1016/j.jhydrol.2010.01.019>
- Yang, Y., Liu, Y., Zhou, M., Zhang, S., Zhan, W., Sun, C., & Duan, Y. (2015). Landsat 8 OLI image based terrestrial water extraction from heterogeneous backgrounds using a reflectance homogenization approach. *Remote Sensing of Environment*, 171, 14–32. <https://doi.org/10.1016/j.rse.2015.10.005>
- Yang, X., Zhao, S., Qin, X., Zhao, N., & Liang, L. (2017). Mapping of urban surface water bodies from Sentinel-2 MSI imagery at 10 m resolution via NDWI-based image sharpening. *Remote Sensing*, 9(6), 596.
- Yao, F., Wang, C., Dong, D., Luo, J., Shen, Z., & Yang, K. (2015). High-resolution mapping of urban surface water using ZY-3 multi-spectral imagery. *Remote Sensing*, 7(9), 12336.
- Yu, Y., Privette, J. L., & Pinheiro, A. C. (2005). Analysis of the NPOESS VIIRS land surface temperature algorithm using MODIS data. *IEEE Transactions on Geoscience and Remote Sensing*, 43(10), 2340–2350. <https://doi.org/10.1109/TGRS.2005.856114>
- Zhang, H., Li, J., Xiang, N., Shen, Q., Zhang, F., & Liang, W. (2014). An automatic method of monitoring water bodies based on GF-1 data. Paper presented at SPIE Ocean Remote Sensing and Monitoring from Space, Beijing, China.
- Zhang, H. G., Lin, Q. Z., Liu, S. H., & Shi, J. C. (2004). Sub-pixel lake mapping in Tibetan Plateau. Paper presented at IEEE International Geoscience and Remote Sensing Symposium, Anchorage, USA.
- Zhang, F., Zhu, X., & Liu, D. (2014). Blending MODIS and Landsat images for urban flood mapping. *International Journal of Remote Sensing*, 35(9), 3237–3253. <https://doi.org/10.1080/01431161.2014.903351>
- Zhou, C. (2000). Flood monitoring using multi-temporal AVHRR and RADARSAT imagery. *Photogrammetric Engineering and Remote Sensing*, 66(5), 633–638.
- Zhu, X., Chen, J., Gao, F., Chen, X., & Masek, J. G. (2010). An enhanced spatial and temporal adaptive reflectance fusion model for complex heterogeneous regions. *Remote Sensing of Environment*, 114(11), 2610–2623. <https://doi.org/10.1016/j.rse.2010.05.032>
- Zhu, W., Jia, S., & Lv, A. (2014). Monitoring the fluctuation of Lake Qinghai using multi-source remote sensing data. *Remote Sensing*, 6(11), 10,457–10,482.